RESEARCH ARTICLE

Characterization, Evolutionary Insights, and Stress-Responsive Expression of the Phosphoenolpyruvate Carboxylase (PEPC) Gene Family in Salix Matsudana

Hui Wei[1,†], **Yi Cao**[1,†], **Xiaoxi Zhou**[1], **Kaixin Sun**[1], **Yuxin Shan**[1], **Tongtong Cao**[1], **Guoyuan Liu**[1], **Bolin Lian**[1], **Fei Zhong**[1], **Jian Shi**[2] **and Jian Zhang**[1,*]

[1] Key Laboratory of Landscape Plant Genetics and Breeding, School of Life Sciences, Nantong University, Nantong 226019, China
[2] Analysis and Testing Center, Nantong University, Nantong 226019, China

Abstract

Phosphoenolpyruvate carboxylase (PEPC) is a vital enzyme in plant carbon metabolism, catalyzing the conversion of phosphoenolpyruvate (PEP) to oxaloacetate (OAA), a key intermediate in numerous biosynthetic pathways. PEPC family members are usually classified into PTPC and BTPC subfamilies, and PTPC subfamily is characterized by a conserved N-terminal serine phosphorylation site, while BTPC lacks this site. In this study, we identified 10 *Salix matsudana PEPC* genes (*SmPEPCs*), which were classified into two subfamilies, PTPC and BTPC, based on phylogenetic tree. Our findings highlighted significant gene duplication events that contributed to the expansion of the SmPEPC gene family, shedding light on its evolutionary development in willow. Comparative synteny analysis with *Arabidopsis thaliana*, *Oryza sativa*, *Populus trichocarpa*, and *S. purpurea* revealed both conserved and diverged patterns of PEPC organization across species. Interaction network analysis, along with Gene Ontology (GO) and Kyoto Encyclopedia of Genes and Genomes (KEGG) enrichment analysis, indicated that *SmPEPCs* are involved in crucial metabolic pathways related to carbon flux. Expression profiling under salt or submergence stress revealed distinct expression patterns of *SmPEPCs*. Specifically, *SmPEPC9* showed predominant upregulation under salt stress, while *SmPEPC6* was mainly upregulated in submergence-tolerant varieties under submergence stress. These results suggested that *SmPEPCs* potentially modulate carbon flux and organic acid metabolism to mitigate stress effects, playing a central role in stress adaptation mechanisms.

Submitted: 15 December 2025
Accepted: 03 January 2026
Published: 17 March 2026

Vol. 1, **No.** 1, 2026.
10.62762/PIJ.2025.111778

***Corresponding author:**
✉ Jian Zhang
yjnkyy@ntu.edu.cn

† These authors contributed equally to this work

Citation
Wei, H., Cao, Y., Zhou, X., Sun, K., Shan, Y., Cao, T., Liu, G., Lian, B., Zhong, F., Shi, J., & Zhang, J. (2026). Characterization, Evolutionary Insights, and Stress-Responsive Expression of the Phosphoenolpyruvate Carboxylase (PEPC) Gene Family in Salix Matsudana. *Plant Innovation Journal*, 1(1), 27–49.

Keywords: Salix matsudana, PEPC, synteny analysis, salt or submergence stress.

1 Introduction

Phosphoenolpyruvate carboxylase (PEPC) is a highly conserved and essential enzyme in plants, algae, archaea, and bacteria, playing a crucial role in carbon metabolism [1, 2]. In plants, PEPC catalyzes the irreversible β-carboxylation of phosphoenolpyruvate (PEP) in the presence of bicarbonate (HCO_3^-) and magnesium (Mg^{2+}) or manganese (Mn^{2+}), generating oxaloacetate (OAA) and inorganic phosphate (Pi) [3, 4]. This reaction is a vital step in carbon fixation, particularly in plants that use C4 and crassulacean acid metabolism (CAM) photosynthetic pathways. In plants, PEPC performs a key role in capturing atmospheric CO_2, converting it into OAA, which then contributes to the synthesis of organic acids like malate [5, 6]. This process not only enhances photosynthetic efficiency but also helps plants adapt to environments with limited water availability or high temperatures by concentrating CO_2 in the chloroplasts during the day, even when stomata are closed [7–9]. In C3 plants, PEPC plays a critical role in replenishing key metabolic intermediates for the tricarboxylic acid (TCA) cycle, allowing plants to sustain various biosynthetic processes, including the production of carbohydrates, proteins, and lipids [10, 11]. The PEPC gene family in plants is typically divided into two major subfamilies based on evolutionary lineage: plant-type PEPC (PTPC) and bacterial-type PEPC (BTPC) [12, 13]. PTPCs are widely distributed in higher plants and are characterized by a conserved N-terminal serine phosphorylation site, which plays a significant role in regulating the enzyme's activity [14, 15]. Phosphorylation of this site enhances PEPC's activity, thus modulating the enzyme's role in carbon fixation and other metabolic processes [10, 16]. On the other hand, BTPCs are generally found in bacteria and some specialized plant species, lacking the serine phosphorylation site that characterizes PTPCs. Despite the conservation of key residues and domains involved in the catalytic reaction and binding with substrates and inhibitors in both PTPC and BTPC, BTPCs appear to function primarily as catalytic and regulatory subunits in specialized class II PEPC heteromeric complexes due to the absence of the unique N-terminal serine phosphorylation motif found in PTPCs [42]. Additionally, BTPCs do not possess this phosphorylation site, they are hypothesized to be regulated through different mechanisms, such as interaction with other proteins or post-translational modifications distinct from those seen in PTPCs [30].

PEPC's functions extend far beyond carbon fixation and metabolism, PEPC also plays a key role in regulating plant responses to environmental stressors [17]. Abiotic stresses such as drought, salinity, and nutrient deficiencies can severely impact plant growth, and PEPC's involvement in mitigating these effects has gained increasing attention [18–20]. In response to drought, overexpressing Agave americana PEPC1 (AaPEPC1) in *Nicotiana tabacum* led to enhanced photosynthetic rates and increased biomass compared to wild-type (WT) plants under normal conditions. These transgenic plants showed increased malate accumulation and enhanced proline biosynthesis, both of which improved the plants' ability to regulate water uptake and better tolerate drought stress. As a result, the transgenic plants showed a significant increase in dry weight and experienced less growth inhibition under drought conditions compared to WT plants. While the control plants died due to drought stress, the transgenic plants survived, demonstrating the potential of AaPEPC1 to improve drought resistance [21]. Additionally, overexpressing maize PEPC in *Arabidopsis thaliana* led to increased PEPC activity compared to control plants. This enhanced PEPC activity facilitated the replenishment of the TCA cycle by providing additional carbon skeletons for amino acid and protein synthesis. Concurrently, proline accumulated in the cytoplasm, helping the plants better manage water uptake and maintain cellular functions under stress. Moreover, malate accumulation played a crucial role under salt stress by neutralizing excess positive charges, reducing cytoplasmic cation concentrations, and stabilizing pH. This coordinated metabolic response, driven by increased PEPC activity, not only supported metabolic processes but also strengthened salt resistance in Arabidopsis [22]. Moreover, submergence significantly increased the abundance of PEPC and heat shock proteins in the root tips of Glycine max [23]. In transgenic *A. thaliana* plants expressing the ascorbate peroxidase (APX) genes from Solanum melongena (SmAPX) and Luffa cylindrica (LcAPX), PEPC expression was notably upregulated after submergence treatment. These transgenic plants also exhibited enhanced submergence tolerance compared to non-transgenic controls. These results suggest that PEPC expression may be induced by the overexpression of SmAPX and LcAPX, playing a role in the plant's response to submergence stress [24].

However, while substantial data exists regarding the

role of PEPC in model plants, the function of PEPC in Salix matsudana, a resilient and economically important willow species, remains largely unexplored. This species is known for its adaptability to various abiotic stresses, yet the underlying molecular mechanisms, including the role of PEPC, remain poorly understood. Therefore, there is a significant knowledge gap regarding how *S. matsudana* utilizes PEPC to cope with environmental stresses, especially when compared to the wealth of data available for model plants. This gap in understanding presents an opportunity to explore the unique regulatory mechanisms of PEPC in *S. matsudana*, which could potentially provide valuable insights for enhancing the stress resilience and ecological performance of this species. Willows, including *S. matsudana*, play crucial ecological roles in riparian zones and are of significant economic importance, particularly in bioenergy production. Given the species' resilience to various environmental stresses, understanding how PEPC mediates stress tolerance through metabolic pathways like carbon flux and organic acid metabolism is critical. These metabolic processes not only impact the plant's survival under adverse conditions but also influence its productivity in bioenergy applications. Therefore, the study of the PEPC gene family in *S. matsudana* (SmPEPC) is of great interest, as it may uncover key regulatory mechanisms that govern both stress adaptation and the species' utility in bioenergy production. In this study, we conducted a comprehensive analysis of the SmPEPC gene family to investigate its role in stress adaptation in *S. matsudana*. We aimed to uncover key regulatory mechanisms involved in carbon metabolism and stress resilience by exploring the evolutionary relationships, gene structures, and functional roles of *SmPEPCs*. Additionally, we examined the expression patterns of these genes under salt and submergence stress to assess their involvement in stress tolerance. Our findings aim to provide insights into how *SmPEPCs* contribute to the plant's metabolic adaptation to environmental challenges and enhance its potential applications in bioenergy production.

2 Methodology

2.1 Genome-wide retrieval and characterization of PEPC gene family in *S. matsudana*

The genome sequence and corresponding general feature format version 3 (GFF3) annotation file for *S. matsudana* were obtained from the NCBI database (accession number: PRJNA687297) [25]. For comparative analysis, the genome data for *A. thaliana*, *Oryza sativa*, *Populus trichocarpa*, and *S. purpurea* were also retrieved from the Phytozome database[1]. The PEPC protein sequences from *A. thaliana*, *O. sativa*, and *P. trichocarpa* (Supplemental Table S1) were used as queries in a BLASTP search against the *S. matsudana* genome to identify putative *SmPEPCs*, setting an E-value threshold of 1e-10. This E-value threshold is commonly used for gene family identification to ensure high sequence similarity and reduce the inclusion of spurious hits. These sequences were further confirmed to contain the PEPCase domain (PF00311) using the Pfam database. All candidate *SmPEPCs* contained the full or essential parts of the PF00311 domain, which is critical for the enzyme's catalytic activity.

To examine the basic physicochemical properties of the identified *SmPEPCs*, ExPASy[2] was used to calculate molecular weight (MW), isoelectric points (pI), aliphatic indices, instability indices, and Grand average of hydropathicity (GRAVY) scores. Subcellular localization predictions for *SmPEPCs* were performed using the Cell-PLoc-2.0 tool [3].

2.2 Phylogenetic analysis, gene structure, and motif identification

Phylogenetic analysis of *SmPEPCs* was performed using the neighbor-joining (NJ) method in MEGA7 software. The NJ method was chosen for its speed and efficiency, which are important for handling the large dataset size. While the maximum likelihood (ML) method is more accurate, NJ is commonly used for large datasets where computational efficiency is prioritized. Protein sequences of PEPCs from *A. thaliana*, Brassica rapa, Glycine max, *O. sativa*, and *S. matsudana* were included to construct a phylogenetic tree. A bootstrap test with 1, 000 replications was applied to assess the reliability of the tree. The gene structure of each SmPEPC was visualized using TBtools software [26], and the distribution of exons and introns was examined based on GFF3 files. To investigate conserved motifs, the multiple expectation maximization for motif (MEME) suite was used to identify conserved sequences in *SmPEPCs*, setting the maximum number of motifs to 10. Motif enrichment analysis was then performed to understand the functional roles of these motifs.

[1] http://phytozome.jgi.doe.gov
[2] https://www.expasy.org/
[3] http://www.csbio.sjtu.edu.cn/bioinf/Cell-PLoc-2/

2.3 Chromosomal localization and synteny analysis

The chromosomal positions of *SmPEPCs* were determined using the GFF3 annotation file from *S. matsudana* genome. These positions were visualized using TBtools software [26] to map the distribution of *SmPEPCs* across the chromosomes and to examine their clustering patterns. For synteny analysis, we examined both intraspecific gene duplications within *S. matsudana* and interspecific synteny with related species. Intraspecific collinearity was analyzed using MCScanX, which identified segmental duplications of *SmPEPCs*. To explore the conservation of *SmPEPCs*, we compared *S. matsudana* with *A. thaliana*, *O. sativa*, *P. trichocarpa*, and *S. purpurea*. The syntenic relationships were visualized to understand the evolutionary conservation of these genes across species. The collinearity was analyzed using MCScanX with the following parameters: Match score = 50, Gap penalty = –1, Match_size = 5, E-value cutoff = 1e-5, Maximum allowed gap = 25, and Overlap window = 5. Additionally, the rates of synonymous (Ks) and nonsynonymous (Ka) substitutions for duplicated *SmPEPCs* were calculated using the Ka/Ks calculator in TBtools.

2.4 Cis-regulatory elements, interaction proteins, GO, and KEGG enrichments

To identify potential cis-regulatory elements in the promoter regions of *SmPEPCs*, the upstream sequences (2, 000 bp) of each identified SmPEPC were retrieved from *S. matsudana* genome using the GFF3 annotation files. These sequences were extracted from the transcription start site (TSS) of each gene. In cases where nearby upstream genes were present, adjustments were made to avoid overlapping promoter regions. These sequences were then analyzed using the PlantCARE online tool to predict the presence of various cis-regulatory elements associated with stress responses, hormonal regulation, and development. Additionally, to investigate potential interaction partners for *SmPEPCs*, a comprehensive protein interaction network was constructed using the STRING database.

Moreover, Gene Ontology (GO) analysis was carried out to gain insights into the functional categories associated with the identified interacting proteins, and GO enrichment analysis was performed using the AgriGO web tool. Kyoto encyclopedia of genes and genomes (KEGG) pathway analysis was performed to explore the metabolic and signaling pathways associated with *SmPEPCs*. KEGG pathways related to carbon metabolism, stress adaptation, and energy production were prioritized to examine the roles of these proteins in the broader metabolic network of *S. matsudana*.

2.5 RNA-sequencing profiling of *S. matsudana* under salt or submergence stress

To explore the molecular mechanisms underlying *S. matsudana*'s response to salt and submergence stress, RNA-sequencing (RNA-seq) was performed on plants exposed to these stresses [27]. For salt stress, *S. matsudana* plants were treated with 200 mM NaCl, and leaf tissues were collected at 4, 8, and 12 h post-treatment. The samples included both salt-sensitive and salt-tolerant varieties, with the salt-sensitive varieties labeled as M0, M4, M8, and M12, and the salt-tolerant varieties as N0, N4, N8, and N12. A total of 24 samples were collected for RNA-seq analysis, and the data were deposited in CNGBdb under the accession number CNP0003817.

For submergence stress, *S. matsudana* plants were submerged in water, and tissue samples were collected at five time points: 0, 4, 12, 24, and 48 h after submergence [28]. The samples were classified into submergence-sensitive (WSYL-CK, WSYL-4h, WSYL-12h, WSYL-24h, WSYL-48h) and submergence-tolerant (WR-CK, WR-4h, WR-12h, WR-24h, WR-48h) groups, resulting in a total of 30 samples. These RNA-seq data were also made available in CNGBdb, with accession number CNP0002062. The gene expression levels were quantified using the fragments per kilobase of transcript per million mapped reads (FPKM) method. Differentially expressed genes (DEGs) were identified based on a log2 fold change (log2FC) of ≥ 1.5 and a false discovery rate (FDR) of <0.01. For read alignment, HISAT2 was used, and featureCounts was employed for gene quantification. Differential expression analysis was performed using DESeq2. These stringent criteria were used to identify genes involved in the stress response, particularly focusing on *SmPEPCs* that could contribute to the plant's ability to cope with salt or submergence stress.

3 Experiments

3.1 Identification and functional characterization of PEPCs in *S. matsudana*

In this study, a total of 11 protein sequences were identified from the *S. matsudana* proteome, including EVM0015793, EVM0042182, EVM0026814, EVM0025673, EVM0032656, EVM0000226,

EVM0001361, EVM0041786, EVM0001631, EVM0003665, and EVM0052543. These sequences were screened using the HMMER profile for the PEPC domain (PF00311), and 10 of these proteins were confirmed as candidates, with the exception of EVM0000226. These 10 *SmPEPCs* were subsequently renamed SmPEPC1 through SmPEPC10 according to their chromosomal locations. Subcellular localization predictions indicated that all *SmPEPCs* are localized in the cytoplasm. The CDS of *SmPEPCs* varied in length from 2394 bp (SmPEPC10) to 3186 bp (SmPEPC8), with the deduced amino acid sequences ranging from 797 aa (SmPEPC10) to 1061 amino acids (SmPEPC8). The MWs of *SmPEPCs* ranged from 88.82 kDa to 119.00 kDa (Supplemental Table S2).

3.2 Phylogenetic analysis and evolutionary classification of PEPCs

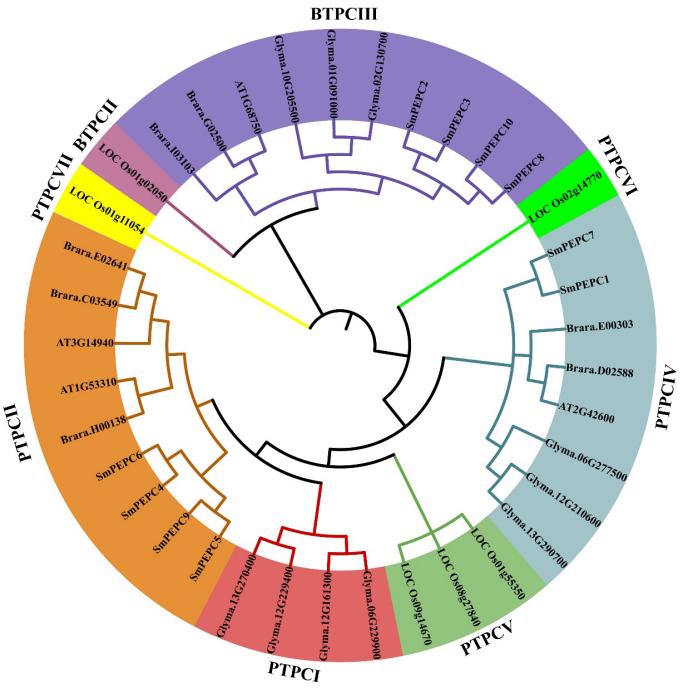

Figure 1. Phylogenetic analysis of *SmPEPCs* and their comparison across different species. This phylogenetic tree illustrated the evolutionary relationships among PEPCs from Salix matsudana (*SmPEPCs*) and other plant species, including *Arabidopsis thaliana*, *Oryza sativa*, Brassica rapa, and Glycine max. The tree was constructed using multiple sequence alignments and the Neighbor-Joining (NJ) method, with the PEPCs grouped into two major subfamilies including PTPC and BTPC. The PTPC subfamily was further subdivided into six distinct clades (PTPCI, PTPCII, PTPCIV, PTPCV, PTPCVI, and PTPCVII), while the BTPC subfamily is divided into two clades: BTPCII and BTPCIII.

To investigate the evolutionary relationships between the *SmPEPCs* and other PEPCs, a phylogenetic tree was constructed using PEPCs from *S. matsudana*, *A. thaliana*, B. rapa, *O. sativa*, and G. max. The resulting dendrogram revealed that PEPCs are clustered into two main subfamilies: BTPC and PTPC (Figure 1). The PTPC subfamily was further subdivided into six distinct clades: PTPCI, PTPCII, PTPCIV, PTPCV, PTPCVI, and PTPCVII, following a nomenclature based on previous studies in plant PEPC phylogenetics [29, 30]. In these studies, the PTPC subfamily was divided into seven groups (PTPCI to PTPCVII), with a distinction between dicot branches and a separate clade formed by monocots, mosses, and ferns. The BTPC subfamily was classified into four groups (BTPCI to BTPCIV) [12]. Within the *SmPEPCs*, three major clades were identified with strong bootstrap support. These clades were classified as follows: PTPCII, which includes *SmPEPC4*, *SmPEPC5*, *SmPEPC6*, and *SmPEPC9*; PTPCIV, which includes SmPEPC1 and SmPEPC7; and BTPCIII, which includes SmPEPC2, SmPEPC3, SmPEPC8, and SmPEPC10. Similar patterns of clade distribution were observed in PEPCs of *A. thaliana* and B. rapa, suggesting conserved evolutionary relationships across these species. Interestingly, *O. sativa* PEPCs were grouped into different clades, namely PTPCV, PTPCVI, PTPCVII, and BTPCII, which diverged considerably from the clade distributions seen in *S. matsudana*, *A. thaliana*, and B. rapa. This suggested that PEPCs from *O. sativa* may have undergone distinct evolutionary processes, leading to their classification in separate clades.

3.3 Exon-intron and conserved motif organization patterns of *SmPEPCs*

The exon-intron structures of *SmPEPCs* were analyzed to gain insights into their genomic organization (Supplemental Figure S1). This analysis revealed considerable variation in the exon-intron arrangements across different *SmPEPCs*, reflecting both their functional diversity and evolutionary history. Based on these exon-intron patterns, the *SmPEPCs* were classified into three major clades: PTPCII, PTPCIV, and BTPCIII. The genes in the PTPCII clade (*SmPEPC4*, *SmPEPC5*, *SmPEPC6*, *SmPEPC9*) displayed relatively complex structures, with larger UTR compared to the genes in the PTPCIV clade. The UTRs of *SmPEPCs* might play a role in post-transcriptional regulation, such as modulating mRNA stability and translation efficiency. In contrast, the BTPCIII clade, which included SmPEPC2, SmPEPC3, SmPEPC8, and SmPEPC10, exhibited a distinct exon-intron organization, characterized by larger introns and exons.

The variation in exon-intron structures among the *SmPEPCs* highlighted their functional specialization and evolutionary divergence.

To investigate functional divergence within *SmPEPCs*, we analyzed the conserved motif compositions of *SmPEPCs* (Supplemental Figure S2). In the PTPCII clade (*SmPEPC4*, *SmPEPC5*, *SmPEPC6*, *SmPEPC9*), the motif composition was highly conserved, with these four members sharing nearly identical patterns. The presence of Motifs 1 through 10 was arranged in a highly similar order across these genes, indicating strong functional constraints. In contrast, the PTPCIV clade (SmPEPC1 and SmPEPC7) retained most of the conserved motifs but exhibited slight variations in the order and relative lengths of motif-containing regions. Notably, SmPEPC1 was missing Motif 7, which further differentiates it from the other members of PTPCII clade. The BTPCIII clade (SmPEPC2, SmPEPC3, SmPEPC8, SmPEPC10) exhibited the greatest divergence in motif arrangement. While the *SmPEPCs* clustered in BTPCIII clade shared a common set of motifs, their positioning was distinct from that of PTPC members. Notably, the spacing between motifs was considerably larger, suggesting a more flexible or diverse functional role within this subfamily compared to the PTPC members.

3.4 Synteny and evolutionary comparison of *SmPEPCs* across plant species

Based on chromosomal positioning, the 10 *SmPEPCs* were randomly distributed across 8 chromosomes of *S. matsudana* and one unplaced contig (Supplemental Figure S3). To further explore the evolutionary dynamics of *SmPEPCs*, we examined their duplication events throughout the willow genome. The analysis revealed that 12 syntenic gene pairs resulted from segmental or whole-genome duplication events (Figure 2). Notably, these collinear gene pairs were confined to the same phylogenetic clade, further supporting the classification of *SmPEPCs* as determined by the phylogenetic tree.

To gain a broader understanding of the collinearity relationships among PEPCs in dicotyledonous plants (*S. matsudana*, *A. thaliana*, *P. trichocarpa*, and *S. purpurea*) and the monocot plant, such as *O. sativa*, we analyzed the syntenic gene pairs across these species (Figure 3). Whole-genome alignments were performed to illustrate the collinearity among the *SmPEPCs*, PtPEPCs, AtPEPCs, OsPEPCs, and SpPEPCs. The results showed stronger homology between *S. matsudana* and dicot plants (*A. thaliana*, *P. trichocarpa*, and *S. purpurea*) than between *S. matsudana* and *O. sativa*. Specifically, 9 syntenic pairs were identified between *S. matsudana* and *A. thaliana*, 14 gene pairs were found between *S. matsudana* and *P. trichocarpa*, and 14 pairs were observed between *S. matsudana* and *S. purpurea*. In contrast, only 2 syntenic pairs were detected between *S. matsudana* and *O. sativa*. These findings suggested that *S. matsudana* exhibits stronger conservation of the PEPC genomic context or microsynteny, particularly *A. thaliana*, *P. trichocarpa*, and *S. purpurea*, than with *O. sativa*. This pattern of collinearity highlighted the conservation of PEPCs in dicots, while indicating that monocots like *O. sativa* might undergone distinct evolutionary processes, leading to differences in gene arrangement and function.

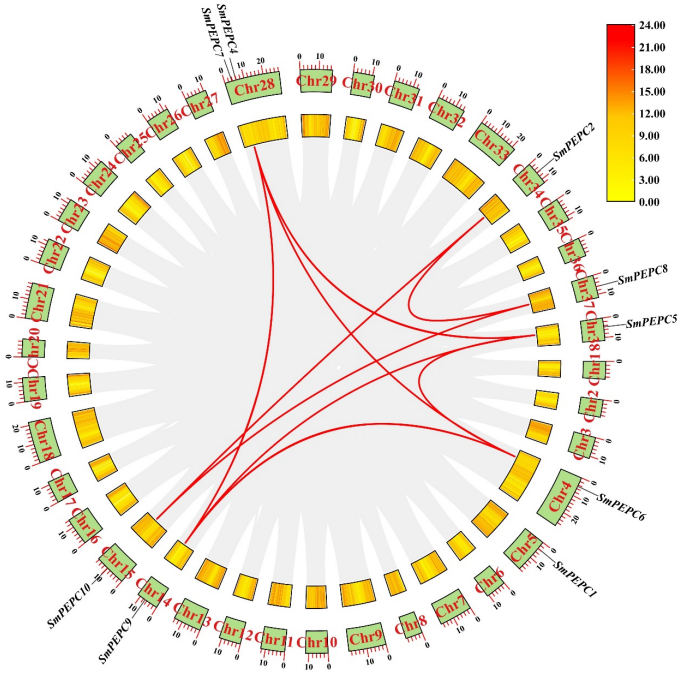

Figure 2. Syntenic gene pairs of *SmPEPCs* in *S. matsudana*. The *SmPEPCs* are located on chromosomes, with each chromosome labeled and represented by blocks along the circle. The red curves indicated syntenic gene pairs between *SmPEPCs* across different chromosomes, reflecting segmental or whole-genome duplication events. In contrast, the gray curves represented all collinear gene pairs across the genome, highlighting the broader syntenic relationships within the *S. matsudana* genome.

3.5 Selection dynamics and evolutionary pressure on *SmPEPCs*

To assess the selective pressures driving the evolution of *SmPEPCs*, we calculated the Ka/Ks ratios for syntenic gene pairs within *SmPEPCs*. The Ka/Ks ratio serves as a key indicator of selective pressure: ratios

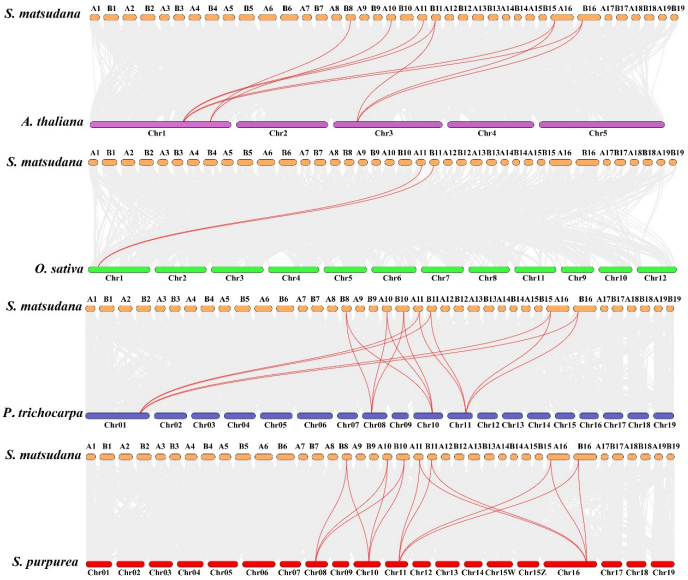

Figure 3. Synteny analysis of *SmPEPCs* across different plant species. The chromosomes of each species were represented in rectangles, with the red curves indicating syntenic relationships between specific SmPEPC gene pairs. Additionally, the gray curves represented all collinear gene pairs across the genomes of the species being compared, highlighting the broader syntenic relationships.

greater than 1 suggest positive selection, ratios less than 1 indicate purifying selection, and ratios equal to 1 imply neutral selection. Our analysis showed that Ka values varied from 0.00337 (*SmPEPC4*/*SmPEPC6*) to 0.0557 (*SmPEPC10*/*SmPEPC3*), while Ks values spanned from 0.0477 (*SmPEPC2*/*SmPEPC3*) to 0.296 (*SmPEPC5*/*SmPEPC6*) (Figure 4 and Supplemental Table S3). The Ka/Ks ratios for these gene pairs were all below 1, indicating that these genes have been subject to purifying selection throughout their evolutionary history.

We also compared the Ka/Ks ratios between *S. matsudana* and *A. thaliana*, *P. trichocarpa*, *S. purpurea*, and *O. sativa* to further investigate the evolutionary dynamics of the PEPC family genes (Figure 5). In the S. *matsudana-A. thaliana* comparison, Ka values, representing the rate of nonsynonymous substitutions, ranged from 0.0696 (*SmPEPC4*/AtPEPC3) to 0.151 (SmPEPC2/AtPEPC4), with these gene pairs exhibiting high sequence divergence (pS $\geq$ 0.75) (Supplemental Table S4). In the S. *matsudana-P. trichocarpa* comparison, Ka values varied between 0.00882 (*SmPEPC5*/PtPEPC5) and 0.0469 (SmPEPC10/PtPEPC3) (Supplemental Table S4). Similarly, in the S. *matsudana-S. purpurea* comparison, Ka values fluctuated between 0.00124 and 0.0541, indicating substantial variation in the rate of functional changes among these gene pairs.

The Ks values, representing the rate of synonymous substitutions, also exhibited considerable variation. In the S. *matsudana-A. thaliana* comparison, Ks values were between 1.328 (*SmPEPC6*/AtPEPC3) and 1.652 (*SmPEPC9*/AtPEPC1). In the S. *matsudana-P. trichocarpa* comparison, Ks values spanned from 0.0788 (*SmPEPC5*/PtPEPC5) to 0.261 (*SmPEPC6*/PtPEPC5), while in the S. *matsudana-S. purpurea* comparison, they varied from 0.0271 (SmPEPC8/Sapur.010G102400) to 0.300 (*SmPEPC6*/Sapur.011G073900) (Supplemental Table S4). These differences in Ks values reflected the varying rates of genetic evolution across these species. The Ka/Ks ratios, which indicate selective pressure, were between 0.0426 (*SmPEPC9*/AtPEPC1) and 0.0985 (SmPEPC2/AtPEPC4) in the S. *matsudana-A. thaliana* comparison, suggesting that these gene pairs are under purifying selection, with deleterious nonsynonymous mutations likely being eliminated. In contrast, the Ka/Ks ratios between *S. matsudana* and *P. trichocarpa* were between 0.0893 (*SmPEPC4*/PtPEPC1) and 0.204 (SmPEPC10/PtPEPC3), while between *S. matsudana* and *S. purpurea*, they ranged from 0.0422 (*SmPEPC5*/Sapur.011G073900) to 0.216 (SmPEPC10/Sapur.010G102400), reflecting differential selective pressures acting on these gene pairs across species. These findings underscored the complex interplay of selective forces shaping the evolution of PEPCs across different plant species. They provided valuable insights into the functional diversification and conservation of PEPCs, revealing evidence of purifying selection in most cases, while also indicating adaptive evolution in certain gene pairs.

3.6 Characterization of cis-regulatory elements in *SmPEPC* gene promoters

The analysis identified a diverse array of cis-regulatory elements associated with plant growth regulation, environmental responses, and hormonal regulation, highlighting the intricate mechanisms that govern SmPEPC gene expression. A significant proportion of CREs were associated with plant growth regulation, accounting for 35.14% of the total elements (Figure 6). Among these, light-responsive elements (LREs) were the most abundant, comprising 25.95%. This high prevalence suggested that light plays a critical role in modulating the expression of *SmPEPCs*, potentially linking their activity to light-driven metabolic processes such as photosynthesis and carbon fixation. This observation was consistent with the

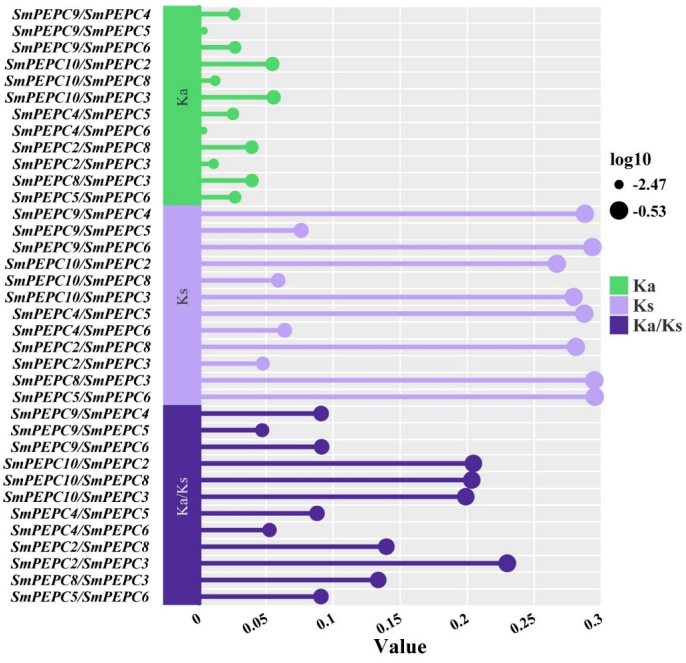

Figure 4. Ka, Ks, and Ka/Ks analysis of SmPEPC gene pairs in *S. matsudana*. The Ka values were represented by green lines, indicating the rate of nonsynonymous substitutions. The Ks values were shown in light purple lines, reflecting the rate of synonymous substitutions. The Ka/Ks ratio was depicted by deep purple lines, serving as an indicator of selective pressure.

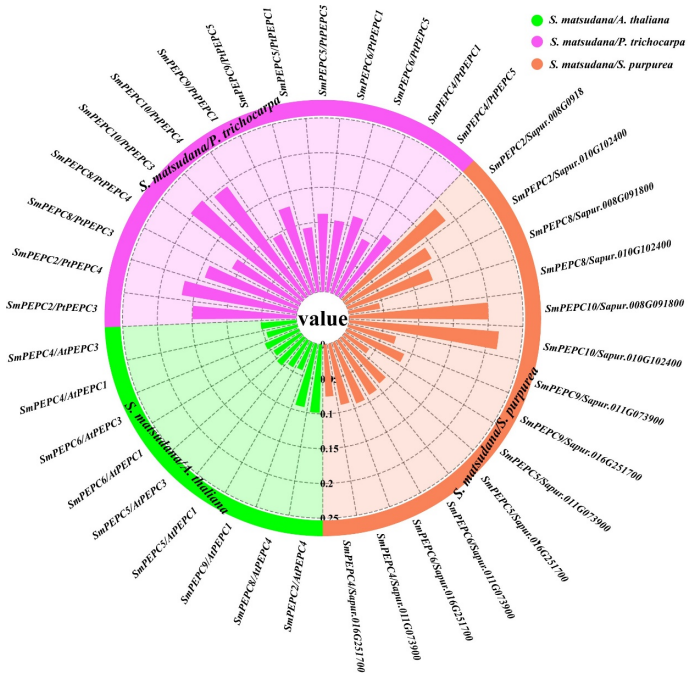

Figure 5. Collinearity analysis of SmPEPC gene pairs in *S. matsudana* and other species. The radial plot presented the syntenic relationships between *SmPEPCs* and their counterparts in other species, with each sector representing a different species' genome. The color-coded segments corresponded to different species: *S. matsudana* and *A. thaliana* (green), *S. matsudana* and *P. trichocarpa* (pink), and *S. matsudana* and *S. purpurea* (orange). The bars indicated the degree of synteny, with longer bars representing stronger collinearity between gene pairs.

known function of PEPCs in photosynthetic carbon fixation.

Additionally, hormone-responsive elements (42.70%) were highly represented in the SmPEPC promoters, with ABA-responsive elements (16.22%) and MeJA-responsive elements (15.14%) being the most prominent (Figure 6). These findings indicated that *SmPEPCs* are likely tightly regulated by key plant hormones, particularly abscisic acid (ABA) and methyl jasmonate (MeJA), both of which are involved in stress responses and growth regulation under various environmental conditions. This suggested that *SmPEPCs* play an important role in mediating plant responses to abiotic stress factors.

In addition to hormone-responsive elements, environment-responsive elements (22.16%) were also present in the promoters, particularly those associated with anaerobic induction (11.35%) and low-temperature responsiveness (6.49%) (Figure 6). These elements further supported the idea that *SmPEPCs* are involved in plant adaptation to abiotic stresses, especially under oxygen deprivation or low-temperature conditions. Other key regulatory elements that govern growth and development were also identified, including MYB binding sites involved in drought-inducibility (3.78%), which further emphasized the role of *SmPEPCs* in responding to developmental cues and environmental challenges, particularly those related to water availability. The frequency of specific cis-regulatory elements in the SmPEPC promoter was compared to the genomic background. This analysis confirms the significant enrichment of light-responsive, hormone-responsive, and environmental-responsive elements in the SmPEPC promoter, supporting the hypothesis that these genes play a crucial role in mediating stress adaptation mechanisms.

Upon further examination of specific *SmPEPCs*, it was found that light-responsive elements were particularly prevalent in the PTPCII clade, including *SmPEPC6*, *SmPEPC4*, *SmPEPC9*, and *SmPEPC5* (Supplemental Figure S4). These genes exhibited significant numbers of LREs, indicating their strong regulation by light, which aligns with their likely roles in photosynthetic processes. The presence of ABA-responsive elements was particularly notable in *SmPEPC4*, *SmPEPC5*, and *SmPEPC9*, suggesting their involvement in

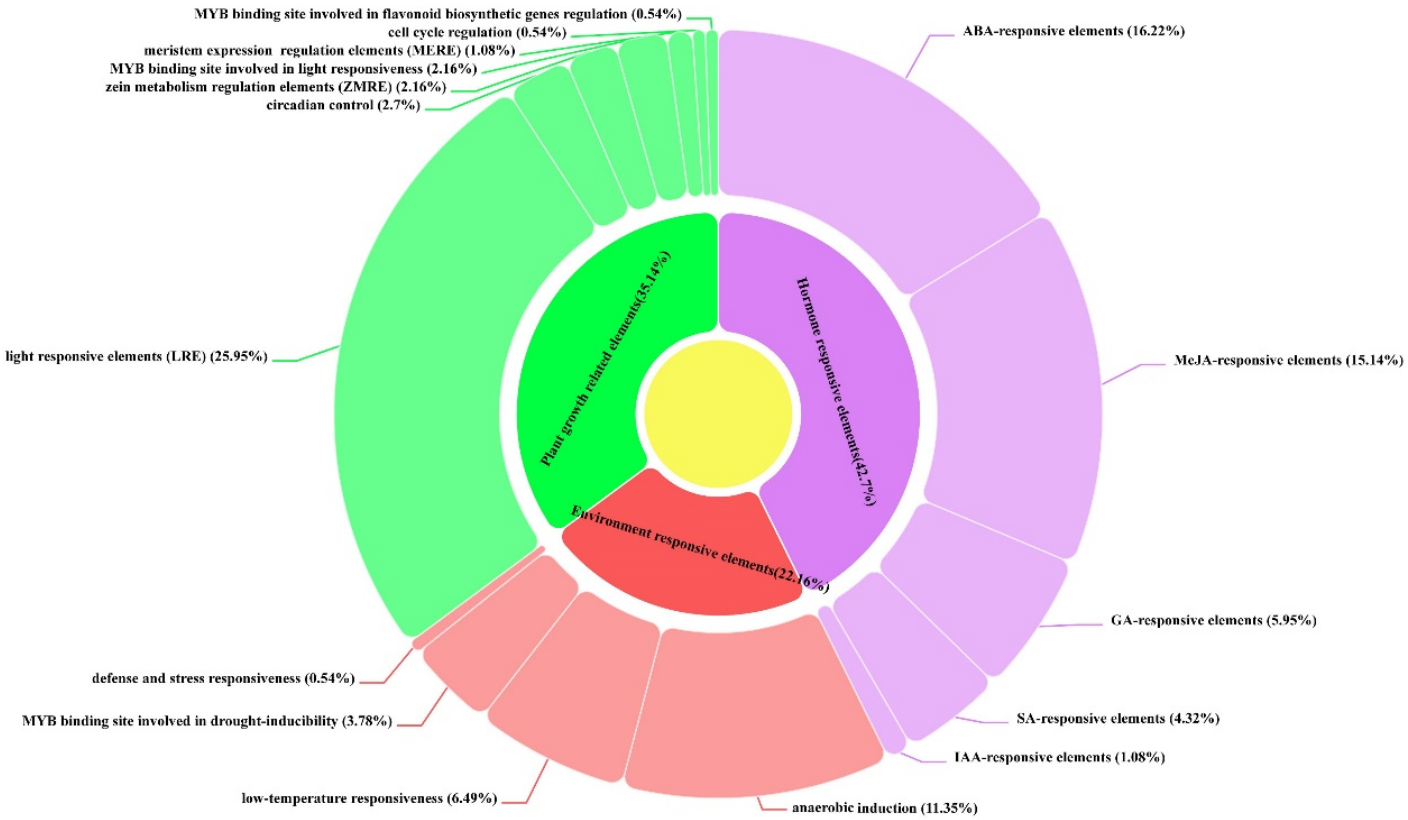

Figure 6. Analysis of cis-regulatory elements in SmPEPC promoters. The circular plot was divided into different segments representing various categories of regulatory elements, with each segment color-coded according to its functional role.

drought and stress responses, as ABA is a key hormone in regulating such responses. Moreover, cell cycle regulation elements were found in *SmPEPC6*, *SmPEPC9*, and *SmPEPC4*, reinforcing the idea that these genes may regulate cellular processes related to growth and division. Together, these findings revealed the complex network of regulatory elements in the promoters of *SmPEPCs*, suggesting that these genes are involved in a broad range of biological processes (BPs), including light-dependent metabolic pathways, stress responses, and growth regulation. The distribution of these regulatory elements across different *SmPEPCs* further suggested that these genes have evolved specialized functions that allow *S. matsudana* to adapt to varying environmental conditions.

3.7 Interactions of *SmPEPCs* with key metabolic proteins

The interaction network of *SmPEPCs* was analyzed to explore their potential interactions with other proteins within the *S. matsudana* genome (Supplemental Figure S5). The interaction map, visualized as a circular diagram, provided a comprehensive overview of how *SmPEPCs* may coordinate their functions with other genomic elements involved in key BPs. The network revealed that *SmPEPCs* are engaged in complex interactions with multiple genes, particularly those involved in metabolic pathways related to carbon metabolism and stress responses. Specifically, there was a robust network of interactions between the *SmPEPCs* and their respective syntenic gene pairs. For example, *SmPEPC4* interacted extensively with proteins such as EVM0043179 (malate dehydrogenase) and EVM0032776 (malate dehydrogenase). This suggested that *SmPEPC4* may work in concert with malate dehydrogenase enzymes in regulating the interconversion of metabolic intermediates, potentially influencing the plant's response to metabolic stress or its carbon fixation efficiency.

Similarly, *SmPEPC5* was connected with several proteins, including EVM0030179 (pyruvate kinase), EVM0052894 (pyruvate kinase), and EVM0057343 (malate dehydrogenase). The interaction between *SmPEPC5* and pyruvate kinase, which was key in glycolysis and energy metabolism, suggested a role for *SmPEPC5* in regulating energy balance and metabolic flux in response to cellular demands. Additionally, interactions with malate dehydrogenase implied that *SmPEPC5* may be involved in maintaining metabolic cycles critical for carbon and nitrogen metabolism. SmPEPC8 also formed several

connections with key metabolic enzymes, including EVM0006298 (malate dehydrogenase), EVM0032028 (malate dehydrogenase), and EVM0013444 (malate dehydrogenase). These interactions further reinforced the potential role of SmPEPC8 in regulating metabolic pathways associated with malate production and energy homeostasis, as malate dehydrogenase was central to the TCA cycle and other metabolic processes. Overall, the interaction network revealed that *SmPEPCs* are not only involved in core metabolic processes but also exhibit a high degree of coordination with other metabolic enzymes, such as malate dehydrogenase and pyruvate kinase. These findings highlighted the complex interplay between *SmPEPCs* and other proteins, suggesting their involvement in key metabolic and regulatory pathways essential for stress response, energy production, and carbon metabolism in *S. matsudana*.

3.8 GO and KEGG enrichment analysis of *SmPEPCs*

The GO enrichment analysis of *SmPEPCs* revealed significant involvement in key BPs and molecular functions (MFs) (Figure 7). The analysis showed that *SmPEPCs* are primarily associated with energy metabolism and carbon fixation. Enriched MFs included carboxy-lyase activity, phosphoenolpyruvate carboxylase activity, and carbon-carbon lyase activity, all of which are vital for processes like photosynthesis and other carbon-related metabolic pathways. In terms of BPs, cellular respiration, tricarboxylic acid cycle, and carbon fixation were significantly enriched, indicating the central role of *SmPEPCs* in energy production and metabolic regulation. The analysis also highlighted the involvement of these genes in primary metabolic processes, reflecting their essential function in cellular metabolism and energy generation. These findings underscored the importance of *SmPEPCs* in regulating critical metabolic and energy pathways, with additional roles in stress response and adaptation mechanisms.

The KEGG enrichment analysis identified key metabolic pathways associated with *SmPEPCs*, highlighting their involvement in energy production, carbon fixation, and carbohydrate metabolism. The most significantly enriched pathway was carbon fixation in photosynthetic organisms (KO: 00710), confirming the role of *SmPEPCs* in carbon fixation during photosynthesis. The pyruvate metabolism pathway (KO: 00620) also showed high significance, indicating the involvement of *SmPEPCs* in pyruvate metabolism, a key step in energy production. Additional enriched pathways included energy metabolism (KO: B09102) and carbohydrate metabolism (KO: B09101), suggesting that *SmPEPCs* contribute significantly to energy production and carbohydrate utilization. Lastly, the broader metabolism category (KO: A09100) was also enriched, further supporting the central role of *SmPEPCs* in regulating metabolic processes. These results emphasized the crucial role of *SmPEPCs* in carbon fixation, energy production, and carbohydrate metabolism in *S. matsudana*.

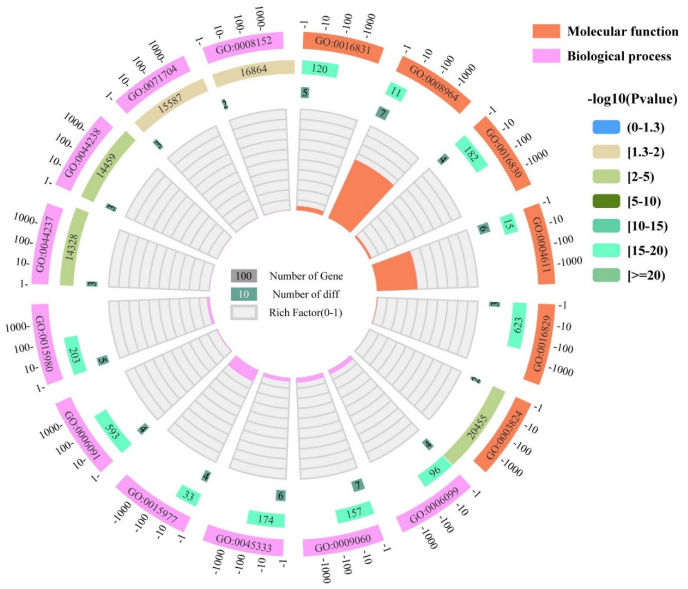

Figure 7. GO enrichment analysis of *SmPEPCs* in *S. matsudana*. The circular plot shows the distribution of GO terms for molecular functions (MFs) (orange) and biological processes (BPs) (pink), with each sector representing a specific GO term. The number of genes associated with each GO term is represented by the color intensity, with darker shades indicating a higher number of genes.

3.9 Salt stress-induced expression patterns of *SmPEPCs* in *S. matsudana*

The expression patterns of *SmPEPCs* reveal distinct differences in the response to salt stress between salt-sensitive (M) and salt-tolerant (N) varieties (Figure 8). Under salt stress, *SmPEPC9* showed a marked upregulation in both the salt-sensitive and salt-tolerant varieties, indicating its potential role as a key salt-responsive gene. Notably, the expression of *SmPEPC9* was significantly higher in the salt-tolerant willow variety at the 12-h time point compared to the salt-sensitive variety, suggesting that *SmPEPC9* may play a crucial role in the salt tolerance mechanisms of *S. matsudana*. This elevated expression

in the salt-tolerant variety highlighted its possible involvement in maintaining cellular homeostasis and mitigating the effects of osmotic stress induced by high salinity.

In contrast, other *SmPEPCs*, including SmPEPC2, SmPEPC3, *SmPEPC4*, *SmPEPC5*, *SmPEPC6*, SmPEPC8, and SmPEPC10, exhibited higher expression levels under normal conditions (0 h) but showed specify downregulation under salt stress. This suggested that these genes might be involved in basal metabolic functions or other growth processes that are downregulated in response to stress. The reduction in their expression upon salt exposure could be part of the plant's adaptive mechanism to prioritize salt stress tolerance-related pathways, such as those regulated by *SmPEPC9*. Overall, the differential expression of *SmPEPCs* under salt stress highlighted the complexity of the plant's response to environmental stressors. While certain genes, like *SmPEPC9*, appeared to be upregulated as part of the salt stress response, others were downregulated, suggesting a coordinated shift in gene expression to optimize resource allocation and enhance salt stress tolerance.

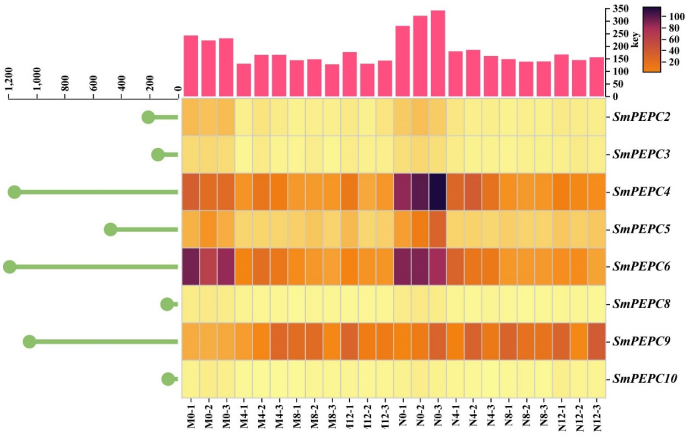

Figure 8. Heatmap of SmPEPC expression under salt stress in *S. matsudana*. The rows represented *SmPEPCs*, while the columns correspond to the different sample groups, with the time points and varieties labeled as M0 (salt-sensitive) and N0 (salt-tolerant), alongside subsequent time points (M4, M8, M12, N4, N8, N12). The color scale indicated the relative expression levels, with darker colors (red) representing higher expression and lighter colors (yellow) corresponding to lower expression.

3.10 Expression profiles of *SmPEPCs* in response to submergence stress

In the WSYL varieties, a marked upregulation of *SmPEPCs*, particularly *SmPEPC9* and *SmPEPC4*, was observed at 24 h (WSYL-24h), indicating a rapid and early response to submergence stress (Figure 9). This suggested that these genes are crucial for the initial stress response and may help the plant cope with the immediate effects of submergence. However, the expression levels of these genes in the salt-sensitive variety decreased over time, potentially indicating a need for the plant to shift to other stress response pathways as it adapted to the prolonged stress. In contrast, the WR willows exhibited a more gradual increase in SmPEPC expression, particularly at the 4-12 h time points, though the increase was significantly lower than that observed in the submergence-sensitive varieties (Figure 9). This more controlled and less dramatic expression pattern in the submergence-tolerant varieties suggested that these plants may activate a more balanced and efficient stress response system, avoiding overactivation of stress genes and potentially conserving energy for long-term stress adaptation.

Moreover, the expression levels of SmPEPC2 and SmPEPC8 in the WR willows were significantly higher compared to the WSYL varieties under stress. This suggested that these genes may play a critical role in helping the plant maintain cellular functions during prolonged submergence, potentially by regulating metabolic processes that are essential for survival under oxygen-deprived conditions. An interesting finding was the expression dynamics of *SmPEPC6*, which might act as a key submergence-response gene (Supplemental Figure S6). Its expression was upregulated at both 24 and 48 h in both the WSYL and WR varieties. However, under the submergence stress, the upregulation of *SmPEPC6* was significantly more pronounced in the WR varieties at the later time points (24-48h). This suggested that *SmPEPC6* may play a critical role in the long-term adaptation to submergence stress, helping the plant maintain metabolic processes and energy balance over extended periods of waterlogging. The WSYL varieties showed a rapid but transient upregulation of certain genes, while the WR varieties exhibit a more stable and sustained expression pattern, especially for genes like *SmPEPC6*, SmPEPC2, and SmPEPC8, which were likely important for long-term stress tolerance and metabolic regulation under prolonged submergence.

3.11 Comparative analysis of *SmPEPC9* and *SmPEPC6* expression in salt or submergence stress

A direct comparison of *SmPEPC9* expression between salt and submergence stress reveals interesting

differences in its induction. While *SmPEPC9* was strongly upregulated under salt stress, especially in the salt-tolerant varieties, its expression in response to submergence stress was less pronounced. Specifically, *SmPEPC9* was more highly induced under salt stress, suggesting its primary role in osmotic stress responses. On the other hand, its response to submergence stress, although still upregulated, was weaker, indicating that *SmPEPC9* may play a more critical role in salt stress adaptation rather than in submergence stress responses. This difference further emphasized the stress-specific roles of *SmPEPC9*, with stronger involvement in salt tolerance mechanisms than in submergence tolerance.

Interestingly, *SmPEPC6* exhibited a distinct expression pattern compared to *SmPEPC9*. *SmPEPC6* was downregulated under salt stress in both salt-sensitive and salt-tolerant varieties, suggesting its involvement in basal metabolic functions that are suppressed during salt stress. In contrast, *SmPEPC6* was strongly upregulated in response to submergence stress, particularly in the submergence-tolerant WR varieties, and this upregulation was more pronounced at the later time points (24–48 h) compared to the earlier time points. This suggested that *SmPEPC6* may play a more critical role in long-term adaptation to submergence stress, particularly in maintaining metabolic processes and energy balance during prolonged periods of waterlogging.

The contrasting expression patterns of *SmPEPC9* and *SmPEPC6* highlighted their stress-specific roles, with *SmPEPC9* primarily involved in salt stress responses, while *SmPEPC6* appeared to be more critical for adaptation to submergence stress. The upregulation of *SmPEPC9* in response to salt stress and the upregulation of *SmPEPC6* in response to submergence stress suggested that these two genes play complementary yet distinct roles in the plant's response to different environmental stressors.

4 Discussion

PEPC plays a key role not only in atmospheric carbon assimilation in C4 and CAM photosynthesis but also in regulating various non-photosynthetic processes. These include guard-cell movement, mineral nutrition, metal tolerance, and fruit acidity [31–33]. Despite these crucial functions, a comprehensive analysis of *SmPEPCs* has not yet been conducted. In this study, we identified 10 *SmPEPCs* within the *S. matsudana* genome, a number that exceeds those found in many

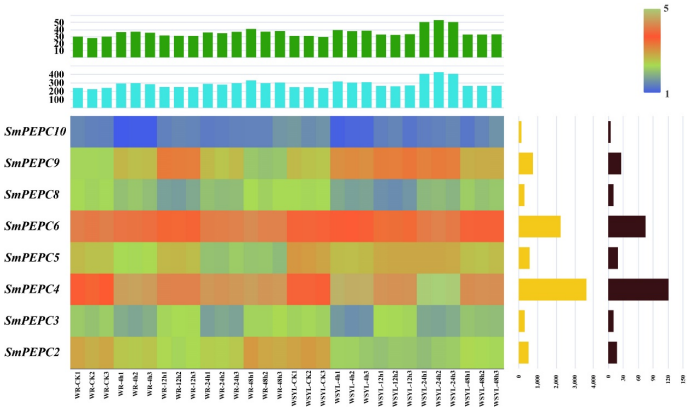

Figure 9. Heatmap of SmPEPC expression under submergence stress in *S. matsudana*. The rows represented *SmPEPCs*, while the columns correspond to the different sample groups, with the time points and varieties labeled as M0 (salt-sensitive) and N0 (salt-tolerant), alongside subsequent time points (M4, M8, M12, N4, N8, N12). The color scale indicated the relative expression levels, with darker colors (red) representing higher expression and lighter colors (yellow) corresponding to lower expression.

other plant species. For comparison, *A. thaliana* has four PEPC genes, *O. sativa* has six, *Zea mays* has six, and *P. trichocarpa* has five [15, 34]. The higher number of *SmPEPCs* in *S. matsudana*, an allopolyploid species, suggests that the duplication events contributing to its polyploid nature may have expanded the PEPC gene family in comparison to these other plants. Typically, PEPCs are categorized into two subfamilies: PTPC and BTPC [35]. Every plant genome sequenced so far contains at least one BTPC member [33]. For instance, Arabidopsis has four PEPCs, comprising one BTPC and three PTPCs. Rice also has six PEPCs, five of which belong to the PTPC subfamily and only one to the BTPC subfamily. Similarly, in *P. trichocarpa*, the PEPCs are classified into two subfamilies: three PTPC members (PtPEPC1, PtPEPC2, PtPEPC5) and two BTPC members (PtPEPC3, PtPEPC4). In line with the PEPC families in Arabidopsis, rice, and poplar, the phylogenetic analysis of *SmPEPCs* in *S. matsudana* also classified them into two primary subfamilies: BTPC and PTPC. Specifically, *SmPEPC4*, *SmPEPC5*, *SmPEPC6*, *SmPEPC9*, SmPEPC1, and SmPEPC7 are grouped into the PTPC subfamily, while SmPEPC2, SmPEPC3, SmPEPC8, and SmPEPC10 are classified under the BTPC subfamily. These findings indicate that, similar to other plant species, the *S. matsudana* PEPC gene family is organized into two distinct subfamilies, PTPC and BTPC, reflecting a conserved evolutionary pattern.

The identification of 12 syntenic gene pairs in *S. matsudana*, resulting from segmental or whole-genome

duplication events, further confirms the genetic restructuring that has occurred in the willow genome. Notably, these collinear gene pairs are confined to the same phylogenetic clade, providing additional support for the classification of *SmPEPCs* as established in the phylogenetic tree. Gene duplication is a well-established mechanism that drives genetic diversity and complexity within plant genomes. Studies by Sánchez et al. [35], Flagel and Wendel [36], and Khan et al. [37] have highlighted that gene duplication events are pivotal for generating evolutionary novelty, leading to the expansion and functional diversification of gene families. In the case of *S. matsudana*, the duplication of *SmPEPCs* likely plays a crucial role in enhancing the plant's ability to respond to various environmental stresses. Gene duplication events can be broadly categorized into two main types: (1) small- or large-scale/whole-genome duplications, which contribute to genome multiplication and speciation, and (2) tandem and segmental duplications, which involve the replication of chromosome fragments and lead to the expansion of gene families [38, 39]. Our analysis of *S. matsudana* supports the occurrence of both segmental and whole-genome duplications, resulting in the formation of syntenic gene pairs and the subsequent expansion of *SmPEPCs*. To explore the evolutionary dynamics of *SmPEPCs*, we compared the syntenic relationships of *S. matsudana* with those of other plants. Our findings revealed stronger homology between *S. matsudana* and dicot species, such as *A. thaliana*, *P. trichocarpa*, and *S. purpurea*, compared to the monocot *O. sativa*. Specifically, 9 syntenic pairs were identified between *S. matsudana* and *A. thaliana*, 14 pairs with *P. trichocarpa*, and 14 pairs with *S. purpurea*. In contrast, only 2 syntenic pairs were found between *S. matsudana* and *O. sativa*. Similarly, previous studies on *P. trichocarpa* PEPCs (PtPEPCs) also revealed similar syntenic relationships across species, with five or four syntenic pairs identified between poplar and Arabidopsis or willow, while no syntenic pairs were detected between poplar and rice [34]. This pattern of differential gene collinearity between dicots and monocots strengthens the idea that dicots, including willow, Arabidopsis, and poplar, share a closer evolutionary relationship in terms of PEPC gene structure and function. Conversely, monocots such as rice have experienced more significant evolutionary divergence, resulting in differences in gene arrangement and function.

Previous studies have highlighted the importance of BTPCs as regulatory subunits that interact with PTPCs to form stable complexes essential for catalyzing various metabolic processes. For instance, BTPC from castor oil seeds has been shown to work in tandem with PTPC to direct carbon from PEP toward acetyl-CoA, thereby regulating the flow of carbon into the TCA cycle and other key metabolic pathways [40]. Similarly, in lilies, the interaction between BTPC and PTPC forms a complex that plays a critical role in regulating metabolic flow during pollen maturation, emphasizing the involvement of PEPC in developmental processes [41]. These studies underscore the sophisticated coordination of metabolic pathways facilitated by the interaction between PTPC and BTPC subunits. In the present study, we observed that *SmPEPCs*, particularly *SmPEPC4* and *SmPEPC5*, engage in significant interactions with key metabolic enzymes such as MDH and PK. Specifically, *SmPEPC4* interacted extensively with malate dehydrogenase, indicating a functional synergy in regulating the interconversion of metabolic intermediates like malate and oxaloacetate. This is consistent with the role of PEPC in the TCA cycle, where malate is a central intermediate. Additionally, the interaction between *SmPEPC5* and pyruvate kinase—an enzyme crucial for glycolysis and energy metabolism—suggests that *SmPEPC5* plays an important role in regulating energy balance and metabolic flux, especially under stress conditions when the plant's energy demands increase. SmPEPC8 also interacted with multiple isoforms of malate dehydrogenase, implying its role in maintaining energy homeostasis through malate production. Given that the TCA cycle is integral to cellular respiration and energy production, the regulation of this cycle by SmPEPC8 and other *SmPEPCs* is likely crucial for *S. matsudana*'s ability to cope with abiotic stresses, which place significant metabolic demands on the plant. These findings are in line with earlier research that suggests PEPC operates within a larger regulatory network that integrates various metabolic pathways. In Arabidopsis, for example, the interaction between PTPC and BTPC was shown to regulate the flow of carbon into the TCA cycle, helping to maintain cellular energy levels and metabolic stability under stress [42, 43]. This highlights the importance of these interactions in enabling plants to adapt to fluctuating environmental conditions, where efficient carbon metabolism and energy balance are essential for survival.

Previous studies have highlighted the central role of PEPCs in plant responses to abiotic stress. For

example, overexpression of maize PEPC in rice enhanced photosynthetic performance under high light and temperature [44]. PEPCs from Arabidopsis, wheat, and sorghum also respond strongly to salt and chilling treatments [45]. In soybean, GmPEPC6/8/9 are markedly induced by cold and salt stress [15]. Likewise, poplar PEPCs, such as PtPEPC4, show increased expression under ABA and oxidative stress at multiple time points [34]. Together, these findings indicate that PEPCs consistently contribute to carbon metabolism adjustment and energy regulation during environmental stress. Consistent with these earlier observations, our analysis of *S. matsudana* revealed that *SmPEPCs* exhibit clear stress-responsive expression patterns under both salt and submergence conditions. Under salt stress, *SmPEPC9* was strongly induced in both salt-sensitive and salt-tolerant varieties, with the latter showing notably higher expression at 12 h. This suggests that *SmPEPC9* is a major salt-responsive gene in *S. matsudana*, potentially helping to stabilize cellular metabolism under osmotic stress. Under submergence stress, *SmPEPC9* and *SmPEPC4* were prominently upregulated in submergence-sensitive varieties at 24 h, implying roles in early oxygen deprivation response. Expression then declined, indicating a likely shift in metabolic strategy as stress duration increased. In contrast, submergence-tolerant varieties displayed more moderate and gradually increasing PEPC expression, suggesting a controlled and energy-efficient adaptive response. Of particular interest was *SmPEPC6*, which showed sustained upregulation in both sensitive and tolerant varieties, with higher induction in tolerant plants at later time points (24–48 h). This pattern suggests that *SmPEPC6* may support long-term metabolic adjustment during prolonged waterlogging, contributing to enhanced submergence tolerance. These results underscore the important roles of *SmPEPCs* in regulating stress responses in *S. matsudana*, particularly under salt and submergence conditions. The differential expression patterns observed between salt-sensitive and salt-tolerant varieties highlight the complex and adaptive nature of SmPEPC gene regulation, with specific genes like *SmPEPC9* and *SmPEPC6* playing pivotal roles in stress tolerance mechanisms

5 Conclusion

In this study, 10 *SmPEPCs* were identified from the *S. matsudana* genome. Phylogenetic analysis revealed that SmPEPC members are classified into the PTPC and BTPC subfamilies, with this classification supported by exon/intron organization and synteny analysis. The analysis of cis-regulatory elements suggested that a large number of putative transcription factors may regulate the expression levels of *SmPEPCs*. Additionally, we characterized a range of proteins interacting with *SmPEPCs*, indicating their essential role in regulating carbon metabolism. GO and KEGG enrichment analyses further suggested that *SmPEPCs* are involved in key metabolic pathways, including carbon fixation, energy production, and stress responses. Moreover, differential expression patterns of *SmPEPCs* were observed in response to salt or submergence stress, with specific genes showing significant upregulation in the salt-tolerant and submergence-tolerant varieties. These findings provide valuable insights into how *S. matsudana* adapts to environmental stresses.

Data Availability Statement

Data will be made available on request.

Funding

This work was supported in part by the Basic Research Program of Jiangsu under Grant BK20250951; in part by the Basic Research Project of Nantong under Grant JC2023104; in part by the Jiangsu Province College Students' Innovation and Entrepreneurship Training Program under Grant 202410304106Y; in part by the Priority Academic Program Development of Jiangsu Higher Education Institutions.

Conflicts of Interest

The authors declare no conflicts of interest.

AI Use Statement

The authors declare that no generative AI was used in the preparation of this manuscript.

Ethical Approval and Consent to Participate

Not applicable.

References

[1] O'Leary, B., Park, J., & Plaxton, W. C. (2011). The remarkable diversity of plant PEPC (phosphoenolpyruvate carboxylase): recent insights

into the physiological functions and post-translational controls of non-photosynthetic PEPCs. *Biochemical Journal, 436*(1), 15-34. [CrossRef]

[2] Lucius, S., & Hagemann, M. (2024). The primary carbon metabolism in cyanobacteria and its regulation. *Frontiers in Plant Science, 15*, 1417680. [CrossRef]

[3] Westers, H., Dorenbos, R., Van Dijl, J. M., Kabel, J., Flanagan, T., Devine, K. M., ... & Quax, W. J. (2003). Genome engineering reveals large dispensable regions in Bacillus subtilis. *Molecular Biology and Evolution, 20*(12), 2076-2090. [CrossRef]

[4] Monreal, J. A., McLoughlin, F., Echevarría, C., García-Mauriño, S., & Testerink, C. (2010). Phosphoenolpyruvate carboxylase from C4 leaves is selectively targeted for inhibition by anionic phospholipids. *Plant Physiology, 152*(2), 634-638. [CrossRef]

[5] Cousins, A. B., Baroli, I., Badger, M. R., Ivakov, A., Lea, P. J., Leegood, R. C., & Von Caemmerer, S. (2007). The role of phosphoenolpyruvate carboxylase during C4 photosynthetic isotope exchange and stomatal conductance. *Plant Physiology, 145*(3), 1006-1017. [CrossRef]

[6] Ludwig, M. (2016). The roles of organic acids in C4 photosynthesis. *Frontiers in Plant Science, 7*, 647. [CrossRef]

[7] Nguyen, T. B. A., Lefoulon, C., Nguyen, T. H., Blatt, M. R., & Carroll, W. (2023). Engineering stomata for enhanced carbon capture and water-use efficiency. *Trends in Plant Science, 28*(11), 1290-1309. [CrossRef]

[8] Tan, B., & Chen, S. (2023). Defining mechanisms of C3 to CAM photosynthesis transition toward enhancing crop stress resilience. *International Journal of Molecular Sciences, 24*(17), 13072. [CrossRef]

[9] Li, C., Wang, J., Lan, H., & Yu, Q. (2024). Enhanced drought tolerance and photosynthetic efficiency in Arabidopsis by overexpressing phosphoenolpyruvate carboxylase from a single-cell C4 halophyte Suaeda aralocaspica. *Frontiers in Plant Science, 15*, 1443691. [CrossRef]

[10] Caburatan, L., & Park, J. (2021). Differential expression, tissue-specific distribution, and posttranslational controls of phosphoenolpyruvate carboxylase. *Plants, 10*(9), 1887. [CrossRef]

[11] Hu, R., Yu, H., Deng, J., Chen, S., Yang, R., Xie, H., ... & Yu, Y. (2025). Phosphoenolpyruvate and related metabolic pathways contribute to the regulation of plant growth and development. *International Journal of Molecular Sciences, 26*(1), 391. [CrossRef]

[12] Cao, J., Cheng, G., Wang, L., Maimaitijiang, T., & Lan, H. (2021). Genome-wide identification and analysis of the phosphoenolpyruvate carboxylase gene family in Suaeda aralocaspica, an annual halophyte with single-cellular C4 anatomy. *Frontiers in Plant Science, 12*, 665279. [CrossRef]

[13] Xu, R., Liu, H., Liu, C., Xia, M., Feng, D., Zhu, Y., ... & Chen, Z. (2025). Genome-wide identification and expression analysis of the PEPC gene family in Zanthoxylum armatum reveals potential roles in environmental adaptation. *Biology, 14*(11), 1605. [CrossRef]

[14] Lepiniec, L., Vidal, J., Chollet, R., Gadal, P., & Crétin, C. (1994). Phosphoenolpyruvate carboxylase: structure, regulation and evolution. *Plant Science, 99*(2), 111-124. [CrossRef]

[15] Wang, N., Zhong, X., Cong, Y., Wang, T., Yang, S., Li, Y., & Gai, J. (2016). Genome-wide analysis of phospho enol pyruvate carboxylase gene family and their response to abiotic stresses in soybean. *Scientific reports, 6*(1), 38448. [CrossRef]

[16] Feria, A. B., Bosch, N., Sánchez, A., Nieto-Ingelmo, A. I., de la Osa, C., Echevarría, C., ... & Monreal, J. A. (2016). Phosphoenolpyruvate carboxylase (PEPC) and PEPC-kinase (PEPC-k) isoenzymes in Arabidopsis thaliana: role in control and abiotic stress conditions. *Planta, 244*(4), 901-913. [CrossRef]

[17] Shaheen, I., Waseem, M., Basharat, S., Pingwu, L., & Qayyum, A. (2025). Bioinformatic identification of phosphoenolpyruvate carboxylase (PEPC) gene family in Brassica napus. *Genetic Resources and Crop Evolution, 72*(5), 5295-5309. [CrossRef]

[18] Zhao, Y., Guo, A., Wang, Y., & Hua, J. (2019). Evolution of PEPC gene family in Gossypium reveals functional diversification and GhPEPC genes responding to abiotic stresses. *Gene, 698*, 61-71. [CrossRef]

[19] Punyasu, N., Kalapanulak, S., & Saithong, T. (2023). CO2 recycling by phospho enol pyruvate carboxylase enables cassava leaf metabolism to tolerate low water availability. *Frontiers in Plant Science, 14*, 1159247. [CrossRef]

[20] Zhang, Z., Zhang, A., Zhang, Y., Zhao, J., Wang, Y., Zhang, L., & Zhang, S. (2024). Ectopic expression of HaPEPC1 from the desert shrub Haloxylon ammodendron confers drought stress tolerance in Arabidopsis thaliana. *Plant Physiology and Biochemistry, 208*, 108536. [CrossRef]

[21] Liu, D., Hu, R., Zhang, J., Guo, H. B., Cheng, H., Li, L., ... & Yang, X. (2021). Overexpression of an agave phosphoenolpyruvate carboxylase improves plant growth and stress tolerance. *Cells, 10*(3), 582. [CrossRef]

[22] Kandoi, D., Mohanty, S., Govindjee, & Tripathy, B. C. (2016). Towards efficient photosynthesis: overexpression of Zea mays phosphoenolpyruvate carboxylase in Arabidopsis thaliana. *Photosynthesis Research, 130*(1), 47-72. [CrossRef]

[23] Komatsu, S., Nakamura, T., Sugimoto, Y., & Sakamoto, K. (2014). Proteomic and metabolomic analyses of soybean root tips under flooding stress. *Protein and Peptide Letters, 21*(9), 865-884. [CrossRef]

[24] Chiang, C. M., Chen, C. C., Chen, S. P., Lin, K. H., Chen,

L. R., Su, Y. H., & Yen, H. C. (2017). Overexpression of the ascorbate peroxidase gene from eggplant and sponge gourd enhances flood tolerance in transgenic Arabidopsis. *Journal of plant research, 130*(2), 373-386. [CrossRef]

[25] Zhang, J., Yuan, H., Li, Y., Chen, Y., Liu, G., Ye, M., ... & Xu, J. (2020). Genome sequencing and phylogenetic analysis of allotetraploid Salix matsudana Koidz. *Horticulture Research, 7*(1), 201. [CrossRef]

[26] Chen, C., Chen, H., Zhang, Y., Thomas, H. R., Frank, M. H., He, Y., & Xia, R. (2020). TBtools: an integrative toolkit developed for interactive analyses of big biological data. *Molecular Plant, 13*(8), 1194-1202. [CrossRef]

[27] Huang, Q., Hua, X., Zhang, Q., Pan, W., Wang, Y., Liu, G., ... & Zhang, J. (2023). Identification and functional verification of salt tolerance hub genes in Salix matsudana based on QTL and transcriptome analysis. *Environmental and Experimental Botany, 215*, 105470. [CrossRef]

[28] Chen, Y., Yang, J., Guo, H., Du, Y., Liu, G., Yu, C., ... & Zhang, J. (2022). Comparative transcriptomic analysis reveals potential mechanisms for high tolerance to submergence in arbor willows. *PeerJ, 10*, e12881. [CrossRef]

[29] Izui, K., Matsumura, H., Furumoto, T., & Kai, Y. (2004). Phosphoenolpyruvate carboxylase: a new era of structural biology. *Annual Review of Plant Biology, 55*(1), 69-84. [CrossRef]

[30] O'Leary, B., Fedosejevs, E. T., Hill, A. T., Bettridge, J., Park, J., Rao, S. K., ... & Plaxton, W. C. (2011). Tissue-specific expression and post-translational modifications of plant-and bacterial-type phosphoenolpyruvate carboxylase isozymes of the castor oil plant, Ricinus communis L. *Journal of Experimental Botany, 62*(15), 5485-5495. [CrossRef]

[31] Ryan, P. R., Delhaize, E., & Jones, D. L. (2001). Function and mechanism of organic anion exudation from plant roots. *Annual Review of Plant Biology, 52*(1), 527-560. [CrossRef]

[32] Heyduk, K., Moreno-Villena, J. J., Gilman, I. S., Christin, P. A., & Edwards, E. J. (2019). The genetics of convergent evolution: insights from plant photosynthesis. *Nature Reviews Genetics, 20*(8), 485-493. [CrossRef]

[33] O'Leary, B., & Plaxton, W. C. (2020). Multifaceted functions of post-translational enzyme modifications in the control of plant glycolysis. *Current Opinion in Plant Biology, 55*, 28-37. [CrossRef]

[34] Wei, H., Lu, Z., Jiang, H., Xue, C., Xu, X., Liu, G., ... & Zhang, J. (2025). Comprehensive analysis of PEPC gene family in Populus trichocarpa: Characterization, evolutionary insights, and the role of PtPEPC4-PtLTPG14 interaction in carbon metabolism. *Plant Physiology and Biochemistry, 220*, 109573. [CrossRef]

[35] Sánchez, R., & Cejudo, F. J. (2003). Identification and expression analysis of a gene encoding a bacterial-type phosphoenolpyruvate carboxylase from Arabidopsis and rice. *Plant Physiology, 132*(2), 949-957. [CrossRef]

[36] Flagel, L. E., & Wendel, J. F. (2009). Gene duplication and evolutionary novelty in plants. *New Phytologist, 183*(3), 557-564. [CrossRef]

[37] Khan, F., Siddique, A. B., Shabala, S., Zhou, M., & Zhao, C. (2023). Phosphorus plays key roles in regulating plants' physiological responses to abiotic stresses. *Plants, 12*(15), 2861. [CrossRef]

[38] Qiao, X., Zhang, S., & Paterson, A. H. (2022). Pervasive genome duplications across the plant tree of life and their links to major evolutionary innovations and transitions. *Computational and structural biotechnology journal, 20*, 3248-3256. [CrossRef]

[39] Wang, Y., Tan, X., & Paterson, A. H. (2013). Different patterns of gene structure divergence following gene duplication in Arabidopsis. *BMC genomics, 14*(1), 652. [CrossRef]

[40] Uhrig, R. G., O'Leary, B., Spang, H. E., MacDonald, J. A., She, Y. M., & Plaxton, W. C. (2008). Coimmunopurification of phosphorylated bacterial-and plant-type phospho enol pyruvate carboxylases with the plastidial pyruvate dehydrogenase complex from developing castor oil seeds. *Plant Physiology, 146*(3), 1346-1357. [CrossRef]

[41] Igawa, T., Fujiwara, M., Tanaka, I., Fukao, Y., & Yanagawa, Y. (2010). Characterization of bacterial-type phosphoenolpyruvate carboxylase expressed in male gametophyte of higher plants. *BMC Plant Biology, 10*(1), 200. [CrossRef]

[42] O'Leary, B., Rao, S. K., Kim, J., & Plaxton, W. C. (2009). Bacterial-type phosphoenolpyruvate carboxylase (PEPC) functions as a catalytic and regulatory subunit of the novel class-2 PEPC complex of vascular plants. *Journal of Biological Chemistry, 284*(37), 24797-24805. [CrossRef]

[43] Park, J., Khuu, N., Howard, A. S., Mullen, R. T., & Plaxton, W. C. (2012). Bacterial-and plant-type phosphoenolpyruvate carboxylase isozymes from developing castor oil seeds interact in vivo and associate with the surface of mitochondria. *The Plant Journal, 71*(2), 251-262. [CrossRef]

[44] Behera, D., Swain, A., Karmakar, S., Dash, M., Swain, P., Baig, M. J., & Molla, K. A. (2023). Overexpression of Setaria italica phosphoenolpyruvate carboxylase gene in rice positively impacts photosynthesis and agronomic traits. *Plant Physiology and Biochemistry, 194*, 169-181. [CrossRef]

[45] Sánchez, R., Flores, A., & Cejudo, F. J. (2006). Arabidopsis phosphoenolpyruvate carboxylase genes encode immunologically unrelated polypeptides and are differentially expressed in response to drought and salt stress. *Planta, 223*(5), 901-909. [CrossRef]

Appendix

A Supplementary Figures

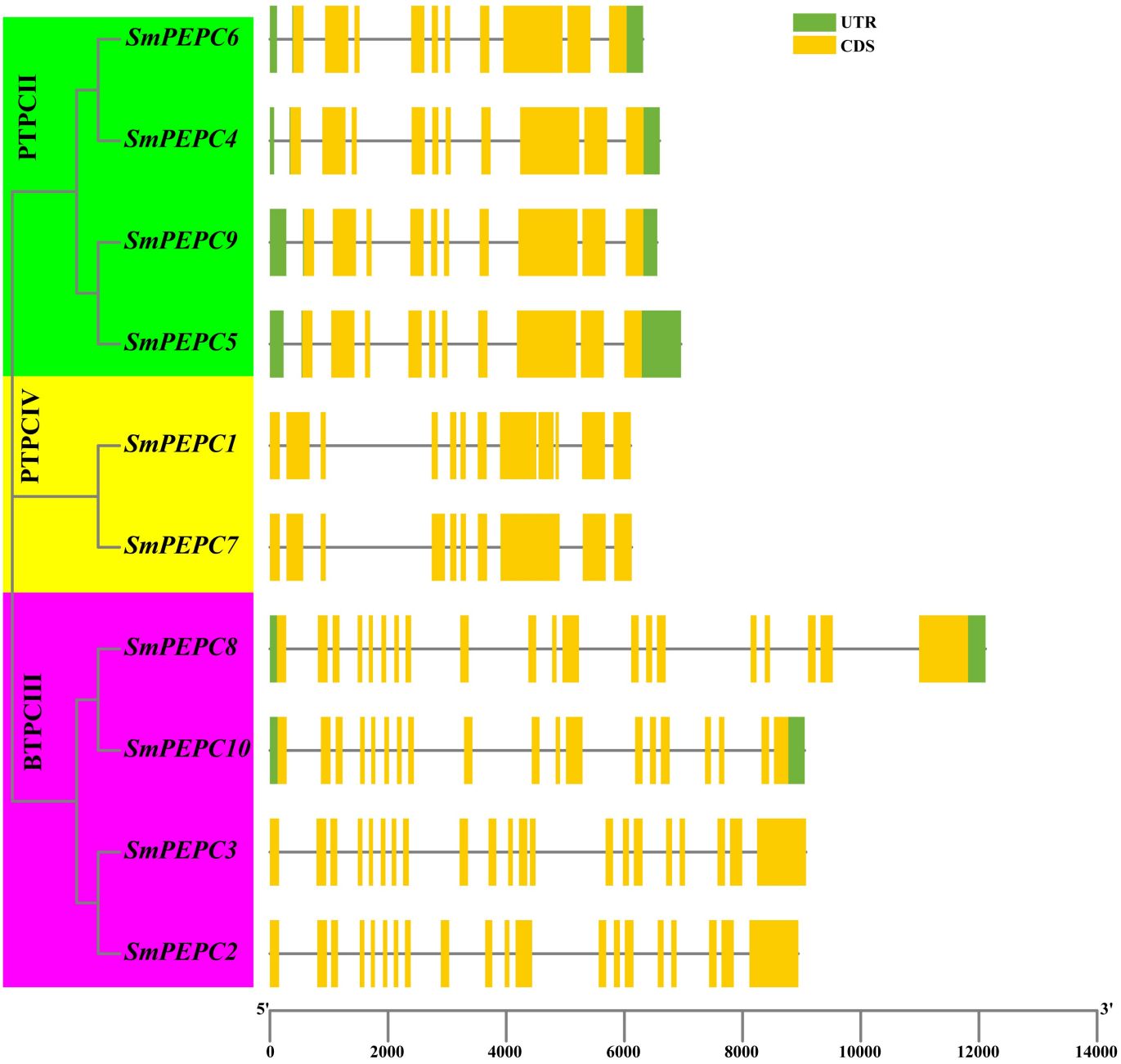

Figure S1. Supplemental Figure A.

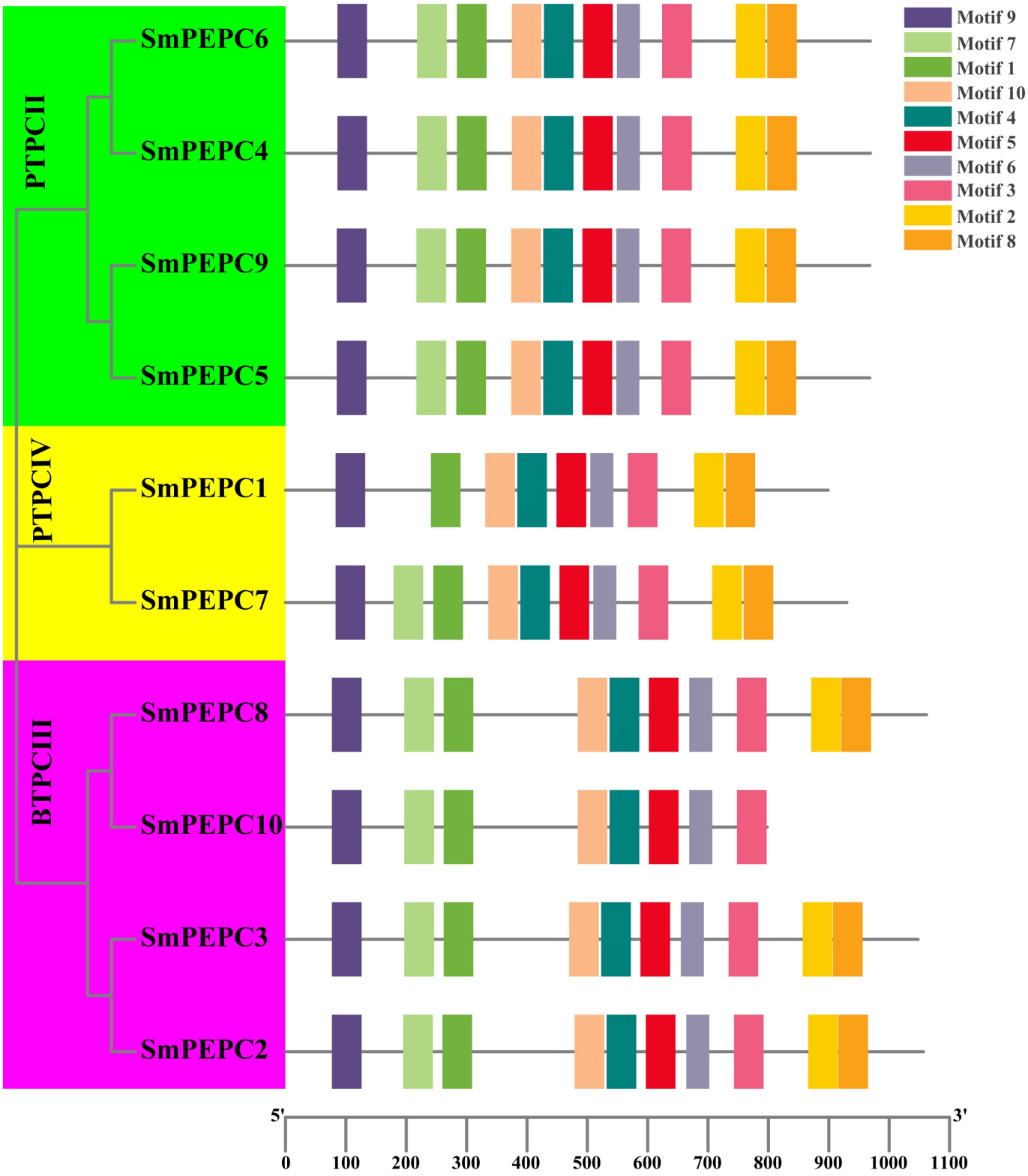

Figure S2. Supplemental Figure B.

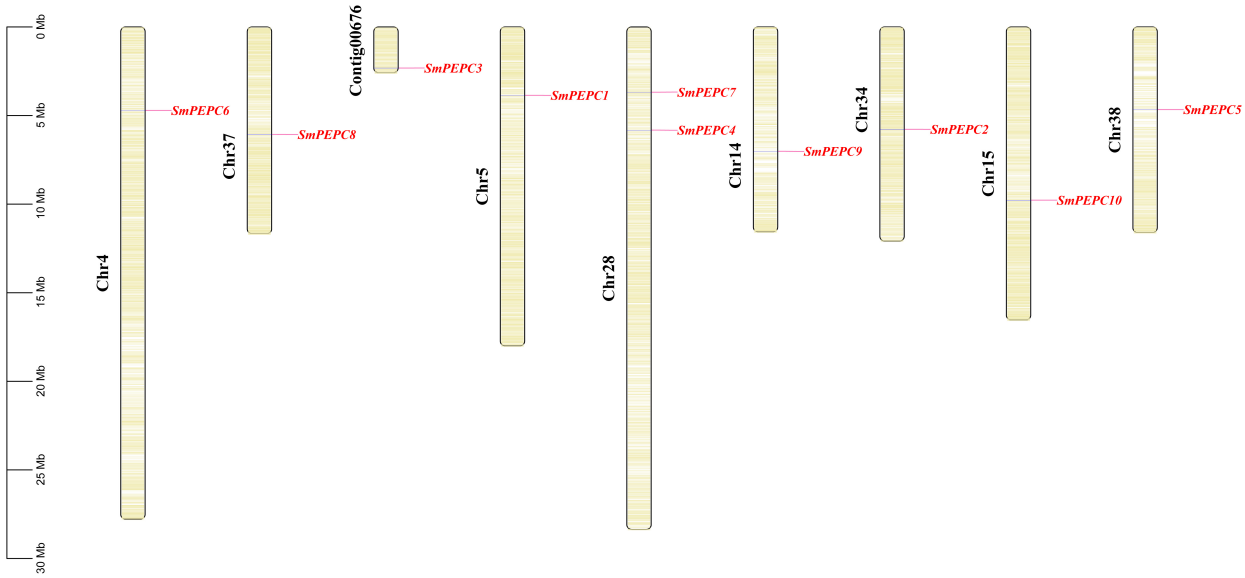

Figure S3. Supplemental Figure C.

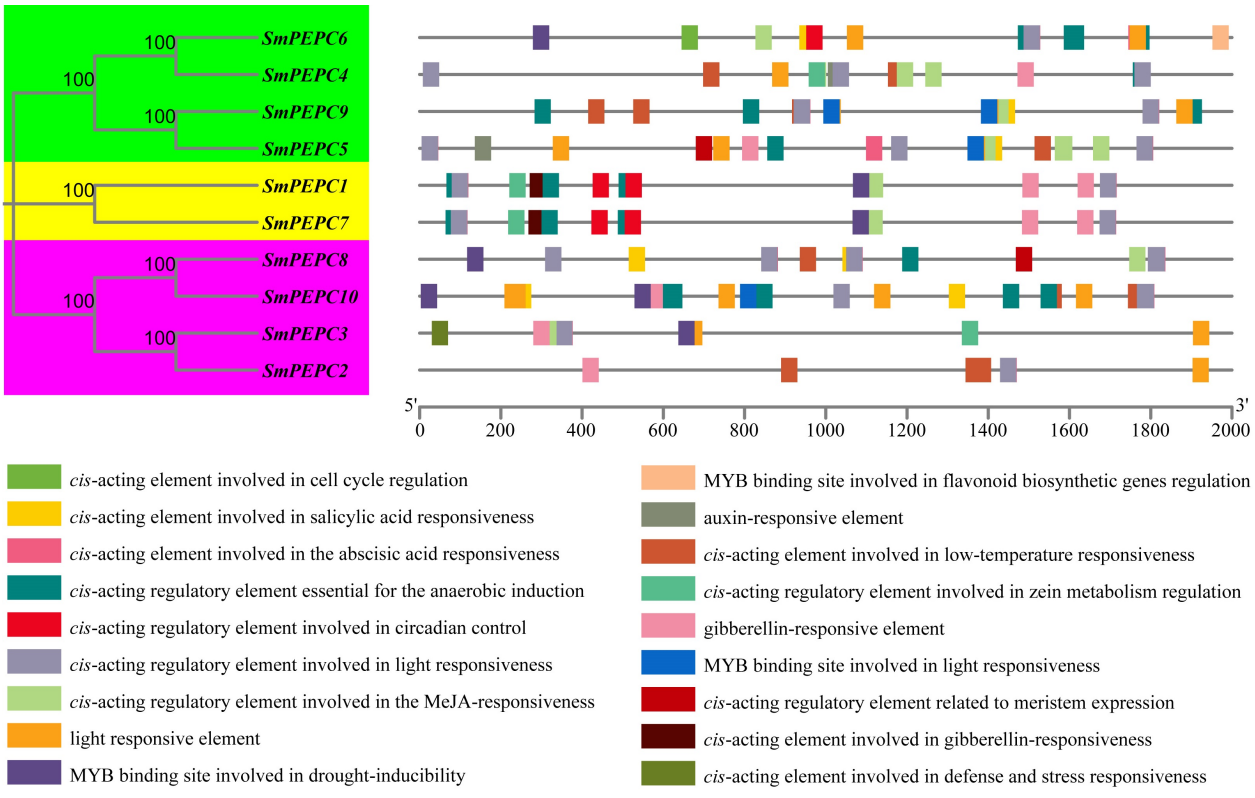

Figure S4. Supplemental Figure D.

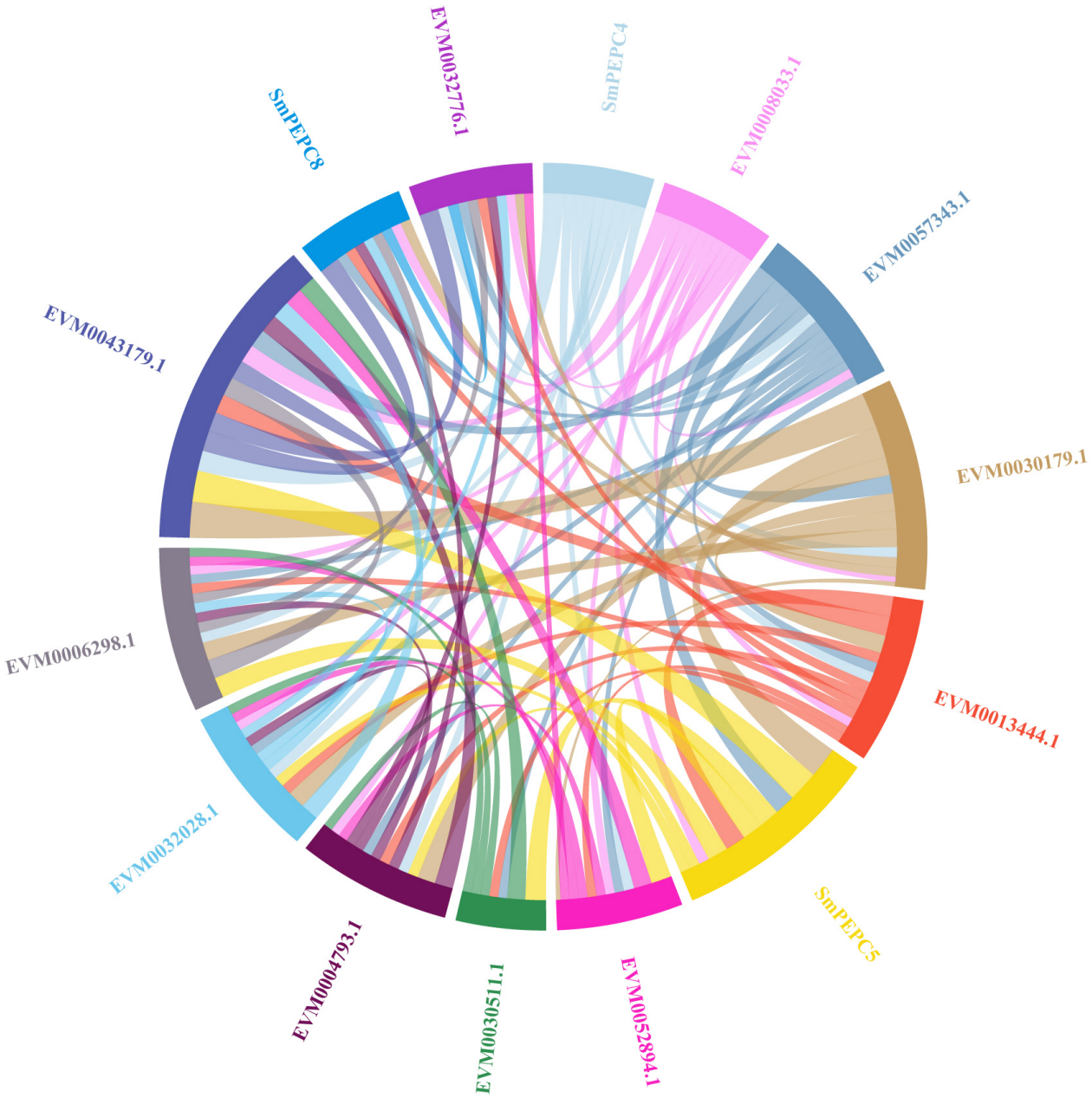

Figure S5. Supplemental Figure E.

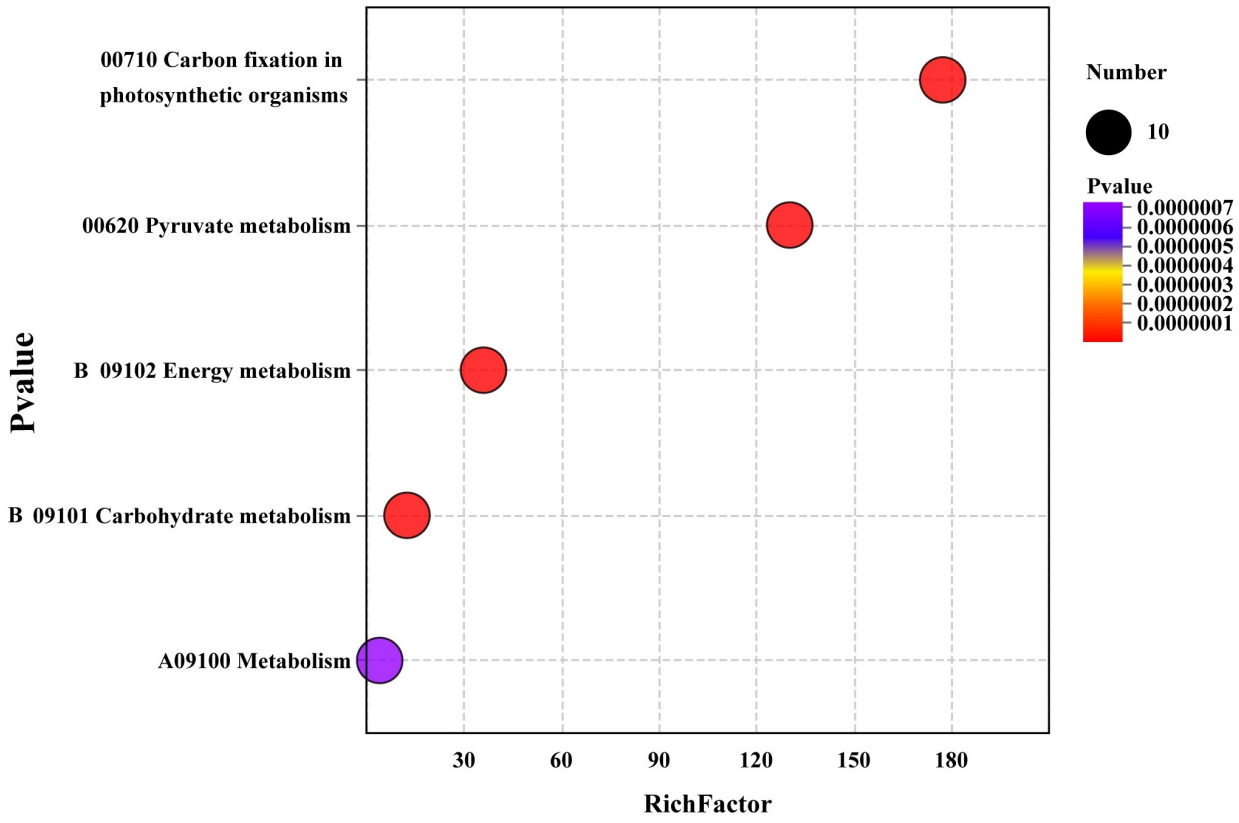

Figure S6. Supplemental Figure F.

B Supplementary Tables

Table S1. Supplemental Table A.

Arabidopsis thaliana		Populus trichocarpa		Oryza sativa
Accession number	Gene Nmae	Accession number	Gene Nmae	Accession number
AT1G53310	AtPEPC1	Potri.001G391900	PtPEPC1	LOC_Os01g02050
AT2G42600	AtPEPC2	Potri.002G214100	PtPEPC2	LOC_Os01g11054
AT3G14940	AtPEPC3	Potri.008G114200	PtPEPC3	LOC_Os01g55350
AT1G68750	AtPEPC4	Potri.010G131800	PtPEPC4	LOC_Os02g14770
		Potri.011G110700	PtPEPC5	LOC_Os09g14670
				LOC_Os08g27840

Table S2. Supplemental Table B.

Gene name	Accession number	CDS length (bp)	Number of amino acid (aa)	Molecular weight (kD)	Theoretical PI	Instability index	Stability	Aliphatic index	Grand average of hydropathicity (GRAVY)	Subcellular localization	Clade
SmPEPC1	EVM0001361	2697	898	102.29	6.13	45.46	unstable	91.14	-0.363	Cytoplasm	PTPCIV
SmPEPC2	EVM0001631	3171	1056	118.99	6.49	50.60	unstable	88.30	-0.438	Cytoplasm	BTPCIII
SmPEPC3	EVM0003665	3144	1047	117.86	6.34	50.68	unstable	87.94	-0.435	Cytoplasm	BTPCIII
SmPEPC4	EVM0015793	2907	968	110.77	5.76	47.01	unstable	89.78	-0.402	Cytoplasm	PTPCII
SmPEPC5	EVM0025673	2904	967	110.43	5.76	46.25	unstable	89.98	-0.409	Cytoplasm	PTPCII
SmPEPC6	EVM0026814	2907	968	110.68	5.70	48.00	unstable	89.89	-0.394	Cytoplasm	PTPCII
SmPEPC7	EVM0032656	2790	929	106.11	6.17	43.76	unstable	90.94	-0.372	Cytoplasm	PTPCIV
SmPEPC8	EVM0041786	3186	1061	119.00	6.16	49.98	unstable	88.44	-0.421	Cytoplasm	BTPCIII
SmPEPC9	EVM0042182	2904	967	110.42	5.79	46.67	unstable	89.88	-0.411	Cytoplasm	PTPCII
SmPEPC10	EVM0052543	2394	797	88.82	5.86	48.66	unstable	86.40	-0.445	Cytoplasm	BTPCIII

Table S3. Supplemental Table C.

Gene Pair		Ka	Ks	Ka/Ks
SmPEPC9	SmPEPC4	0.0262864	0.2881583	0.0912221
SmPEPC9	SmPEPC5	0.0036028	0.0763304	0.0472001
SmPEPC9	SmPEPC6	0.0269101	0.2938489	0.0915780
SmPEPC10	SmPEPC2	0.0547727	0.2673049	0.2049071
SmPEPC10	SmPEPC8	0.0120555	0.0591727	0.2037339
SmPEPC10	SmPEPC3	0.0557430	0.2798184	0.1992115
SmPEPC4	SmPEPC5	0.0253661	0.2877252	0.0881609
SmPEPC4	SmPEPC6	0.0033742	0.0640245	0.0527018
SmPEPC2	SmPEPC8	0.0393976	0.2815355	0.1399383
SmPEPC2	SmPEPC3	0.0109734	0.0476629	0.2302286
SmPEPC8	SmPEPC3	0.0395307	0.2952846	0.1338732
SmPEPC5	SmPEPC6	0.0269203	0.2955961	0.0910714

Table S4. Supplemental Table D.

Gnne Pair		Ka	Ks	Ka/Ks	Note
SmPEPC2	AtPEPC4	0.151076221	1.533587896	0.098511615	
SmPEPC8	AtPEPC4	0.14755723	1.589129548	0.092854123	
SmPEPC9	AtPEPC1	0.070345597	1.652369485	0.042572559	
SmPEPC5	AtPEPC1	0.070125759	1.563469574	0.044852654	
SmPEPC5	AtPEPC3	0.071051319	1.358421092	0.05230434	
SmPEPC6	AtPEPC1	0.072690542	1.537533678	0.047277366	
SmPEPC6	AtPEPC3	0.070652018	1.328152285	0.053195721	
SmPEPC4	AtPEPC1	0.071689275	1.57475832	0.045523985	
SmPEPC4	AtPEPC3	0.069652758	1.347049382	0.05170765	
SmPEPC9	LOC_Os01g11054	0.17404885	NaN	NaN	High Sequence Divergence Value (pS=0.75)
SmPEPC5	LOC_Os01g11054	0.172976949	NaN	NaN	High Sequence Divergence Value (pS=0.75)
SmPEPC2	PtPEPC3	0.0173539	0.116030442	0.149563335	
SmPEPC2	PtPEPC4	0.040242455	0.24024159	0.167508276	
SmPEPC8	PtPEPC3	0.034531203	0.244200847	0.141404928	
SmPEPC8	PtPEPC4	0.014127842	0.127473618	0.110829533	
SmPEPC10	PtPEPC3	0.04686373	0.229340384	0.20434138	
SmPEPC10	PtPEPC4	0.026149075	0.133499326	0.195874208	
SmPEPC9	PtPEPC1	0.024429524	0.25198399	0.096948717	
SmPEPC9	PtPEPC5	0.010643295	0.08219897	0.129482092	
SmPEPC5	PtPEPC1	0.02351075	0.251614897	0.093439422	
SmPEPC5	PtPEPC5	0.008824297	0.078794139	0.11199179	
SmPEPC6	PtPEPC1	0.011079908	0.107084014	0.103469297	
SmPEPC6	PtPEPC5	0.029984491	0.260631202	0.115045667	
SmPEPC4	PtPEPC1	0.009485935	0.106274058	0.089259181	
SmPEPC4	PtPEPC5	0.028422041	0.25725907	0.11048023	
SmPEPC2	Sapur.008G091800	0.010402025	0.055484564	0.187476021	
SmPEPC2	Sapur.010G102400	0.040286692	0.286941288	0.14040047	
SmPEPC8	Sapur.008G091800	0.037683652	0.291413191	0.129313474	
SmPEPC8	Sapur.010G102400	0.001235076	0.027078753	0.045610535	
SmPEPC10	Sapur.008G091800	0.05410652	0.270157361	0.200277794	
SmPEPC10	Sapur.010G102400	0.013174396	0.061014221	0.215923368	
SmPEPC9	Sapur.011G073900	0.00224913	0.031794845	0.070738829	
SmPEPC9	Sapur.016G251700	0.026200877	0.291051828	0.090021346	
SmPEPC5	Sapur.011G073900	0.003151856	0.074663337	0.042214245	
SmPEPC5	Sapur.016G251700	0.02528094	0.292798317	0.086342503	
SmPEPC6	Sapur.011G073900	0.02737906	0.300314906	0.091167836	
SmPEPC6	Sapur.016G251700	0.002697339	0.028664708	0.09409966	
SmPEPC4	Sapur.011G073900	0.026754866	0.298979357	0.089487336	
SmPEPC4	Sapur.016G251700	0.005177868	0.068969574	0.075074675	

Hui Wei has dedicated his research to the genetic improvement and stress resistance of woody plants such as willows and poplars. He has achieved numerous significant results and accumulated extensive practical experience in the fields of plant genomics, molecular biology, and other cutting-edge research areas. He has published several high-impact academic papers in renowned international journals, including Horticulture Research, Annals of Botany, Plant Science, and Industrial Crops and Products. (Email: weihui2021@ntu.edu.cn)

Jian Zhang is a prominent researcher specializing in the molecular regulatory mechanisms of stress resistance in landscape plants and the enhancement of forest ecological carbon sequestration. His work also explores the interaction mechanisms between forest trees and microorganisms in challenging environments. With expertise in molecular biology, genetics, cell biology, and gene engineering, combined with advanced multi-omics sequencing approaches, he investigates the mechanisms underlying unique traits of plants and their potential applications in carbon sequestration. His research provides critical technical support for molecular-assisted breeding of landscape plants and the enhancement of carbon sequestration in forestry. (Email: yjnkyy@ntu.edu.cn)